Schizophrenia Research 240 (2022) 1–21

Contents lists available at ScienceDirect

Schizophrenia Research

journal homepage: www.elsevier.com/locate/schres

Structural covariance networks in schizophrenia: A systematic review Part I

Konasale Prasad [a,b,c,*], Jonathan Rubin [d], Anirban Mitra [e], Madison Lewis [b], Nicholas Theis [a], Brendan Muldoon [a], Satish Iyengar [e], Joshua Cape [e]

[a] University of Pittsburgh School of Medicine, Western Psychiatric Institute and Clinic, 3811 O'Hara St, Pittsburgh, PA 15213, United States of America
[b] University of Pittsburgh Swanson School of Engineering, 3700 O'Hara St, Pittsburgh, PA 15213, United States of America
[c] VA Pittsburgh Healthcare System, University Dr C, Pittsburgh, PA 15240, United States of America
[d] Department of Mathematics, University of Pittsburgh, 301 Thackeray Hall, Pittsburgh, PA 15260, United States of America
[e] Department of Statistics, University of Pittsburgh, 1826 Wesley W. Posvar Hall, Pittsburgh, PA 15260, United States of America

ARTICLE INFO

Keywords:
Schizophrenia
Connectome
Structural covariance network
Graph theory

ABSTRACT

Background: Schizophrenia is proposed as a disorder of dysconnectivity. However, examination of complexities of dysconnectivity has been challenging. Structural covariance networks (SCN) provide important insights into the nature of dysconnectivity. This systematic review examines the SCN studies that employed statistical approaches to elucidate covariation of regional morphometric variations.

Methods: A systematic search of literature was conducted for peer-reviewed publications using different keywords and keyword combinations for schizophrenia. Fifty-two studies met the criteria.

Results: Early SCN studies began using correlational structure of selected regions. Over the last 3 decades, methodological approaches have grown increasingly sophisticated from examining selected brain regions using correlation tests on small sample sizes to recent approaches that use advanced statistical methods to examine covariance structure of whole-brain parcellations on larger samples. Although the results are not fully consistent across all studies, a pattern of fronto-temporal, fronto-parietal and fronto-thalamic covariation is reported. Attempts to associate SCN alterations with functional connectivity, to differentiate between disease-related and neurodevelopment-related morphometric changes, and to develop "causality-based" models are being reported. Clinical correlation with outcome, psychotic symptoms, neurocognitive and social cognitive performance are also reported.

Conclusions: Application of advanced statistical methods are beginning to provide insights into interesting patterns of regional covariance including correlations with clinical and cognitive data. Although these findings appear similar to morphometric studies, SCNs have the advantage of highlighting topology of these regions and their relationship to the disease and associated variables. Further studies are needed to investigate neurobiological underpinnings of shared covariance, and causal links to clinical domains.

1. Introduction

Dysconnectivity among key brain regions rather than single regional pathology is proposed to underlie schizophrenia. We mean "dysconnection/dysconnectivity" as impairments/malfunctioning of the connections/connectivity in contrast to disconnection/disconnectivity, which refers to an absence of connections among regions (Stephan et al., 2009). Examining dysconnectivity is challenging because of the complexities in the qualitative nature of dysconnectivity, quantifying the degree of deviation from the norm, and causally linking dysconnectivity with the disease and its manifestations. These challenges are compounded for in vivo neuroimaging data because of poor spatial and temporal resolutions.

Structural magnetic resonance imaging, diffusion weighted imaging (DWI) and functional magnetic resonance imaging (fMRI) are extensively used to investigate dysconnectivity. Structural covariance networks (SCNs) constructed using regional volumes, cortical thickness, gyrification, and surface area can capture patterns of covariation of brain regions within and between subjects. Investigation of SCNs using these measures is supported by replicated differences in brain morphometry between schizophrenia and healthy subjects and their association with clinical variables. GM volume alterations have been

* Corresponding author at: 3811 O'Hara St, Pittsburgh, PA 15213, United States of America.
E-mail address: kmp8@pitt.edu (K. Prasad).

https://doi.org/10.1016/j.schres.2021.11.035
Received 15 March 2021; Received in revised form 2 August 2021; Accepted 23 November 2021
Available online 11 December 2021

associated with delusion severity (Prasad et al., 2004a; Prasad et al., 2004b), prognosis (Dazzan et al., 2015; Mitelman et al., 2003; Prasad et al., 2005), and neurocognitive impairments in schizophrenia (Czepielewski et al., 2017), healthy subjects (Goodkind et al., 2015), and subjects at-risk for psychosis (Cannon et al., 2015; Prasad et al., 2010). More than 50 regions have showed reduced volumes (Shenton et al., 2001), cortical thickness (Padmanabhan et al., 2015) and surface area (van Erp et al., 2018) while some have shown larger volumes, e.g., putamen (Ellison-Wright et al., 2008). Meta-analyses have reported inconsistent gray matter (GM) loss across the regions (Chan et al., 2011; Ellison-Wright et al., 2008; Honea et al., 2005; Steen et al., 2006; Vita et al., 2006) although some were more consistently altered, e.g., anterior cingulate cortex (ACC) and insula (Chan et al., 2011; Ellison-Wright et al., 2008). These inconsistencies may be attributed to differences in methodologies, MRI data, illness duration and medications.

DWI measures anisotropy of water diffusion from which diffusion metrics (e.g., fractional anisotropy, radial diffusivity) are calculated indexing white matter (WM) integrity and diffusion stream count. These metrics can reveal an altered "wiring diagram" at the macroscale or mesoscale. Structural connectivity partly explains how brain regions interact to affect behavioral output. Functional connectivity that involves correlation of time-series of hemodynamic data reflecting synchronous hemodynamic response among nodes can further inform behavioral manifestations. Since the correspondence between functional and WM connections is generally low, ranging between 0.3 and 0.5 (Suarez et al., 2020), understanding structural topology can help in better qualitative appreciation and quantitative estimation of dysconnectivity. This review will focus on SCNs and their implications for understanding the pathophysiology of schizophrenia.

SCNs can highlight topology of brain structures that can be analyzed to reveal hierarchical brain organization, intrinsic cortical organization, and mutual influence of changes in regional measures. These features are replicated at both individual and population levels, which is a clear advantage of examining SCNs (Alexander-Bloch et al., 2013). Between-group comparison using regions-of-interest (ROI) or voxel-based morphometry (VBM) approaches cannot provide such data. Further, SCNs of the human brain significantly differs from random networks (Bullmore and Sporns, 2009, 2012) suggesting that the shared variations of brain regions are not random. This is supported by prior studies that reported greater between-subject variability of regional volumes compared to between-subject differences in whole-brain volume (Kennedy et al., 1998) and that between-subject differences in one region frequently covary with between-subject differences in other regions (Lerch et al., 2006).

Examination of such covariance in schizophrenia began almost as soon as MRI was deployed to investigate the brain biology of schizophrenia. Widespread use of neuroimaging, computation-based morphometric parcellations and applications of advanced mathematical and statistical approaches have enabled examination of covariance structure of multiple brain regions. The focus of this review is to discuss

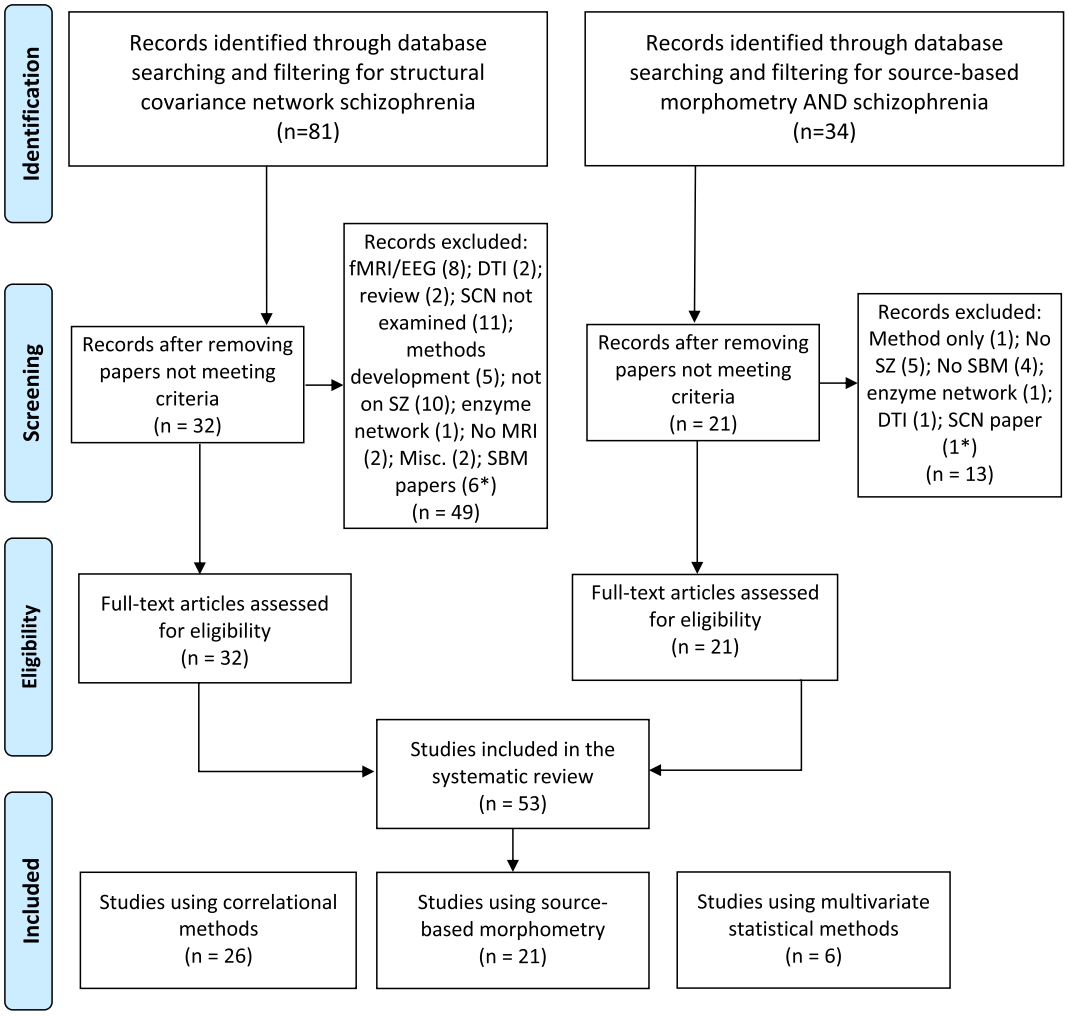

Fig. 1. PRISMA 2009 Flow Diagram.
*These studies were included in the other bin.

what has been learned about covariation of brain regions so far, to summarize evolving methodologies, to clarify the biological and pathophysiological significance of SCN to schizophrenia, and to chart future directions.

2. Methods

The PubMed, PsychInfo and Embase databases were searched using different keywords and combinations for peer-reviewed papers published until July 04, 2021, yielding a number of papers: "structural covariance" ($n = 11{,}159$), "structural covariance network" ($n = 1274$) and "structural covariance network AND schizophrenia" ($n = 80$), "structural covariance AND schizophrenia" ($n = 316$), "morphometric covariance" ($n = 495$), "morphometric covariance AND schizophrenia" ($n = 26$), "source based morphometry" ($n = 262$), "source based morphometry AND schizophrenia" ($n = 33$) (Fig. 1). Citations within these papers were also searched. The inclusion criteria were that the manuscripts should: (a) be published in a peer-reviewed journal, (b) address schizophrenia, (c) describe image acquisition, processing, and statistical/mathematical procedures, and (d) compare with appropriate healthy subjects.

Sixty-eight published studies that examined SCN using either statistical or mathematical approaches met the inclusion criteria. To adequately deal with these two approaches, this review is divided into two parts. Part I will describe 53 studies using statistical methods to build and analyze the SCNs. Part II will describe the studies that used graph theoretic approaches along with studies that examined persons at risk for schizophrenia.

3. Results

3.1. Statistical methods used in structural covariance studies

Statistical approaches were the mainstay until the mid-2000s after which mathematical approaches using graph theory gained popularity. Selected statistical approaches are described. Some studies relied mainly on correlational approaches, but recent studies have applied multivariate approaches.

Correlations: Although the SCN is called a covariance network, the networks are built using correlations. Correlation and covariance both quantify the relationship of variations in two variables, but correlation is normalized to vary between −1 and 1 whereas covariance is not. Suppose there are morphometric measures of ROIs for n subjects, i.e., n observations on cortical thickness at each ROI. Correlation coefficients are calculated for each pair of ROIs giving one group-level network for each group. Networks can be thresholded to examine binary networks consisting of binary edges. The Pearson, Spearman, or partial correlations have been used to study networks. Along with the property of positive semi-definiteness, a correlation network provides a measure of similarity between ROIs. The SCNs can then be examined using various statistical procedures (Table 1).

Source-based morphometry (SBM) is a data-driven algorithm which provides a multivariate extension to VBM using independent components analysis (ICA). SBM does not require a priori region selection. After preprocessing using VBM to create voxelwise map of GM concentration/volume or WM measures at each voxel, the voxels from the 3D image are unwrapped into a single row. ICA is applied to a subject-by-voxel GM or WM matrix resulting in a loading matrix and component matrix. The rows of the component matrix and columns of the loading matrix are then considered in pairs. The component rows indicate how one component contributes to different brain voxels. *t*-tests can be performed on each column of loading coefficient to examine which components show group difference among the loading components (Table 2).

Principal Components Analysis (PCA) is a dimension reduction technique used to find a few principal directions, or weighted linear combinations of measurements, that explain most of the variability in data. Given N sample observations on p variables, first the sample covariance matrix is calculated, and then mutually orthogonal eigenvectors or principal directions are recorded. In an SCN, the data may consist of the observations from N subjects on p ROIs. The first principal component (PC) is computed by the dot product between the first eigenvector and the observations on the subject, leading to N observations on the first PC. The next PCs are computed using the same procedure. Orthogonality ensures that the r^{th} PC is uncorrelated with the previous $r - 1$ PCs and the first PC represents a direction along which measurements exhibit maximum variance; the second PC maximizes variance over directions orthogonal to the first PC and so on. This process is also used in Principal Components Regression (PCR) where, given observations on a response variable and predictor variables, the desired number of PCs are calculated and used to predict the response through linear regression. Predictors measured in different units should be standardized to calculate eigenvectors of the correlation matrix instead of covariance matrix.

Partial Least Squares (PLS) Regression is based on PCA but overcomes the unsupervised approach of PCR. The PCs of the predictor variables are used instead of the predictors themselves to predict the response variable. However, the directions that best explain the predictors may not be the best directions to predict the response (James et al., 2013). The problem of response variables not contributing to the dimensionality reduction in PCR is alleviated by the supervised approach of PLS regression. Given response variable Y and features $X_1, \cdots, X_p$ the first PLS direction is computed as $U_1 = \sum_{i=1}^{p} \phi_{1i} X_i$, where ϕ_{1i} are the regression coefficients obtained by regressing Y on X_i for each i separately. Next, each X_i is regressed on U_1 and the residuals are recorded and interpreted as the unexplained information from the first PLS direction. In place of the original predictors, these residuals are used in a similar fashion to compute the second PLS direction, U_2, and so on. The number of directions is chosen usually via cross-validation. In both PCA and PLS, bias decreases with increasing number of dimensions but variance increases. In SCN, PLS correlation (PLSC) is considered. Two matrices X, Y are considered where X is a matrix of brain activity and for seed-based PLSC, Y is a matrix of voxel intensities. A singular value decomposition $R := X^\top Y = U \Lambda V^\top$ is computed where the matrices of left singular vectors U and right singular vectors V are called silences (Krishnan et al., 2011; Spreng et al., 2019).

Granger Causality (GC) has been successfully adopted into neuroscience to study the causal effect of one time series on another. Suppose y_t is an auto-regressive time series of order p and one wishes to test if another time series x_t Granger-causes y_t. Then the following model,

$$y_t = \alpha_0 + \alpha_1 y_{t-1} + \cdots + \alpha_p y_{t-p} + \beta_q x_{t-q} + \cdots + \beta_r x_{t-r} + \epsilon_t$$

is formed, where ϵ_t is white noise and r > q. F-tests are then used to check which of the lagged values of x_t survive. If all the coefficients $\beta_q, \cdots, \beta_r$ fail to be significant, then it is said that x_t does not Granger-cause y_t. Thus, when GC is detected, it implies that knowledge of x_t is helpful in the future prediction of y_t (Table 3).

3.2. Structural covariance studies

3.2.1. Studies examining selected brain regions

Early studies examined the fronto-temporal regions. Shenton et al. (1992) reported both positive and negative correlations of GM volumes among several regions within the temporal lobe in patients. Breier et al. (1992) examined the GM and WM volumes of the prefrontal cortex (PFC), caudate and limbic regions and reported correlations between the prefrontal WM and limbic GM volumes among patients. Neither study found significant correlations among controls. Wible et al. (1995) replicated Shenton et al. (1992) findings. By including PFC GM and WM, replicated Breier et al. (1992) results, and also found covariations among controls. Bullmore et al. (1998) reported positive correlations in

Table 1
Structural covariance network studies on schizophrenia and related psychotic disorders that used statistical approaches to build the networks.

	Authors	Study Sample and goals	Methods	Main findings
Correlation-based SCN				
1	Raucher-Chéné et al. (2020)	110 patients with SZ and 72 HC Examined SCNs of SZ patients classified into low ToM and high ToM groups, in comparison with HC. To find association of alterations in SCN with ToM constructs by comparing low ToM and high ToM groups between each other and with HC	3 Tesla MRI with 1 mm slice thickness processed using the Freesurfer and parcellated based on the Desikan-Killiany-Tourville atlas for regional surface area. Covariance across surface area of 12 ROIs after regressing age, sex, and total brain surface area constructed in one model for group comparison without IQ as an additional covariate. A second model including IQ as an additional covariate. A third model added medication effect as another covariate to the above	Stronger covariance between the right rostral middle frontal gyrus and the right superior temporal gyrus in SZ compared to HC in both models. Low ToM group showed stronger covariance between the right caudal middle frontal gyrus and the left middle temporal gyrus than in the high ToM group in the first model. The second model that added IQ as an additional covariate showed stronger covariance between left caudal middle frontal gyrus and the right superior temporal gyrus in the low ToM than in the high ToM group, in addition to the above regions. Third model that included medication effect as an additional covariate showed stronger covariance in two additional nodes: left caudal middle frontal gyrus and the right middle temporal gyrus in low compared to high ToM group, and left middle temporal gyrus and the left superior temporal gyrus in high compared to low ToM group
2	Zhang et al. (2020)	107 first episode SZ and 92 HC Structural integrity differences between the two groups on 8 selected networks, namely auditory, sensorimotor, visual, speech, semantic, executive, salience, and default networks	After data extraction from these regions using 4 mm radius spheres, independent correlation networks were built separately for each group. GM volume of the sphere is used as a covariate of interest in independent correlation analysis	"Structural association" differences (the slope of the SCN differences between SZ and HC) were found within the auditory and executive control networks. Auditory regions showed positive correlations in controls but negative or no correlations among patients. For the executive control network, SZ showed positive correlation and HC showed negative or no correlations
3	Moberget et al. (2018)	983 SZ spectrum disorders and 1349 HC from 14 international centers. Cerebello-cerebral structural covariance of cerebellar regional volumes with cortical thickness. Examined the group differences between cerebellar volumes.	This was a mega-analysis of cerebellar volume followed by voxel-wise cerebello-cerebral structural covariance analysis. Uncorrected t-maps for case-control comparisons	Total cerebellar gray matter volume was robustly reduced in SZ relative to HCs (Cohen's $d = -0.35$), with the strongest effects in cerebellar regions showing functional connectivity with frontoparietal cortices ($d = -0.40$) Positive correlations between cerebellar volume and cerebral cortical thickness in frontotemporal regions (i.e., overlapping with areas that also showed reductions in SZ) that showed reduced volumes in schizophrenia.
4	Kuang et al. (2017)	15 first-episode psychosis patients and 15 HC Relationship of cognitive insight with VLPFC seed based SCN of cortical thickness using the Mapping Anatomical Correlations Across the Cerebral Cortex (MACACC)	Seed-based structural covariance was examined using Pearson correlation tests using the VLPFC as a seed with all other cortical areas.	No significant differences between patients and controls on either the left or the right VPPFC seed-based cortical thickness SCN Self-certainty but not self-reflectiveness showed positive association with medial PFC and pars triangularis
5	Buchy et al. (2017)	15 early psychosis and 15 historical controls Goal was to conduct an exploratory SCN analysis.	3 Tesla MRI data acquired at 1 mm thickness. Seed-based structural covariance examined through regression models using the Mapping Anatomical Correlations Across the Cerebral Cortex (MACACC) Modulation of structural covariance by facial emotion recognition examined.	Reduced covariance was observed in early psychosis compared to controls in the right fusiform face area and the right orbitofrontal cortex area. Negative effect of emotion differentiation accuracy on structural covariance between left fusiform face area and right supramarginal gyrus
6	Zalesky et al. (2015)	109 childhood onset SZ, 86 of their unaffected siblings and 102 HC. To examine longitudinal developmental trajectory of corticocortical connectivity from 12 to 24 years	MRI data acquired on a 1.5 Tesla GE scanner using the 3D SPGR protocol at 1.5 mm slice thickness. Pearson correlations were used to investigate covariance of cortical thickness for regions defined on the DKT atlas that were then summed into coarse-grained regions such that there were 5 regions on each hemisphere (frontal, parietal, temporal, occipital and cingulate). Regional thickness was used after regressing age, sex, socioeconomic status, vocabulary-scaled score, and total GM volume from the thickness estimates. Connectivity mapped at every other year from 12 to 24 years.	Correlation of cortical thickness between the left occipital cortex and left temporal lobe was reduced in patients from 12 to 22 years compared to controls. Between the ages of 16 and 20 years, connectivity between the right occipital cortex and left temporal lobe was decreased in patients compared to controls that failed to reach significance by early adulthood. Siblings of patients showed similar pattern including the left occipital to left temporal lobe correlations. Left occipitotemporal correlations in patients were significantly reduced in the group with high Scale for Assessment of Positive Symptoms (SAPS) scores; low SAPS group did not show significant differences.
7				

(*continued on next page*)

Table 1 (*continued*)

	Authors	Study Sample and goals	Methods	Main findings
	Wheeler et al. (2014)	54 SZ patients aged 18–55 years and 68 HC matched for age, sex, handedness, and highest parental level of education. The goal was to examine the relationship of altered structural coupling between cortical regions with cognitive performance.	T1-weighted MRI acquired on a 1. 5 Tesla GE Echospeed system using 8-channel head coil. Used a vertex-wise approach to compare brain-wide cortical thickness correlations in SZ patients and HC using regions of reduced thickness identified in the study sample. Thickness was residualized for age.	Cortical thinning was observed in the frontal, temporal, and parietal lobe along with the subcortical regions. Vertices in these regions were selected as the seeds. Of the 18 seeds, one in the DLPFC showed significant differences in cortical thickness correlations with other regions in SZ compared to controls at 5% FDR where SZ patients showed higher left-right correlations than controls. SZ patients scoring below the median on letter number sequence test showed stronger and more widespread thickness correlations but not for executive function as measured on Trails B test. HC, also, showed stronger correlations in subjects scoring below the median for letter number sequence scores.
8	Chen et al. (2014b)	86 First Episode SZ and 86 age and gender matched HC To examine association of regional GM volume with SZ and covariation of selected regions	3 Tesla MRI data acquired at 1 mm thickness. 16 ROIs selected based on a meta-analysis (Ellison-Wright et al., 2008) and the current study were defined as spherical areas with variable radius (20 mm radius for uncus/ amygdala and 10 mm for other ROIs) Linear regression to regress out the effects of age, sex, and intracranial volume after which they were included in a correlation matrix.	Insula and amygdala bilaterally and postcentral gyrus were different between patients and controls. Intra- and inter-insula, inter-amygdala, and insula–parietal connections showed difference in covariation between patients and controls
9	Clos et al. (2014)	BrainMap metadata Goal was to examine to what extent resting state, meta-analytic connectivity modeling and SCN elucidate the commonalities, differences and interactions between SCN and functional connectivity.	A database of published functional and structural neuroimaging studies that have reported Talairach or MNI coordinate based results. Seed-based SCN and functional connectivity (resting state and meta-analytic connectivity modeling) data by using the anterior insula as the seed	All three approaches (SCN, resting state and meta-analytic) showed significant dysconnectivity of left anterior insula with several brain regions; however, the strongest dysconnectivity was with the neighboring nodes extending into the inferior frontal cortex and supplementary motor cortex. Conjunction analysis showed 3 regions common to all 3 analyses: bilateral anterior insula extending to inferior frontal gyrus, precentral gyrus, and posterior medial frontal cortex. Each individual analyses revealed different functional implications.
10	Collin et al. (2013)	146 early course SZ and 122 HC Main goal of the study was to explore patterns of GM coupling in SZ.	1.5 Tesla MRI data with 1.2 mm slices Freesurfer package to obtain global GM volume, cerebral gray and white matter volume and ventricular volumes. Total of 82 cortical and subcortical volumes were used derived from the Desikan-Killiany-Tourville atlas (Desikan et al., 2006). Pearson correlations of GM volumes corrected for age, sex and total GM volume followed by permutation tests for inter-regional and inter-lobar coupling. Network based statistics (NBS) was used to compare the groups for inter-regional coupling. NBS involves creating a binary difference matrix by comparing the SZ and HC matrices and masking the SZ matrix using consistently identified correlations based on bootstrapping in HC sample. Largest connected component was identified and then permuted to rule out a component as purely by chance. Permutation tests were used to compare interlobar connections while network based statistics (NBS) were used to compare the inter-regional networks (Zalesky et al., 2010).	33 interlobar connections were statistically different from 0 in controls. SZ patients showed both increased (L. temporal and bilateral subcortical, and the left and right frontal lobes, and left frontal and left limbic GM volume) and decreased (L. frontal and bilateral subcortical GM volumes) inter-lobar coupling. In the inter-regional between lobar GM volumes two subnetworks of abnormal coupling were identified: one with 12 and another with 8 regions. Larger subnetwork had nodes with higher coupling in patients compared to controls in frontal to limbic (parahippocampal gyrus and anterior cingulate), L. temporal and occipital lobes, and between lateral temporal/parietal and limbic regions. Larger subnetwork with decreased coupling in patients compared to controls was observed in prefrontal and posterior cortical regions (left pericalcarine sulcus, right superior parietal gyrus) and between regions in the medial temporal lobe and right fronto-limbic regions. Smaller subnetwork with 8 nodes showed higher coupling in patients than controls between supramarginal to pallidum, and to bilateral thalamus. Smaller subnetwork also showed decreased coupling in patients in supramarginal to post-central, post-central to inferior frontal, and anterior cingulate to inferior frontal opercular part of GM compared to controls.
11	Abbs et al. (2011)	29 females and 59 males with SZ compared to 21 female and 27 male HC. Main goal was to examine neuroanatomical underpinnings of sex differences in verbal memory in SZ.	1.5 Tesla MRI data at 3.1 mm coronal slices. Selected regions associated with verbal memory that show morphometric abnormalities in schizophrenia and sexual dimorphisms were examined, namely anterior cingulate, PFC, hippocampus, parahippocampal gyrus and	Female SZ patients showed significant covariance. Differences between hippocampus and anterior cingulate gyrus, inferior parietal lobule and PFC, and inferior parietal cortex and anterior cingulate cortex compared with female HC. Male

(*continued on next page*)

Table 1 (*continued*)

	Authors	Study Sample and goals	Methods	Main findings
			inferior parietal cortex. Correlation tests were used	SZ patients and HC did not show such significant covariance differences. Volumes in male SZ patients were reduced across all regions in the network consisting of the hippocampus, parahippocampal gyrus, PFC, and inferior parietal cortex. Female patients showing significant covariance is interpreted as greater variability in volumetric reductions in female patients. Hippocampus and PFC volumes were significantly related to memory performance in males, which was poorer than in female patients
12	Modinos et al. (2009)	26 patients with medication resistant hallucinations. No healthy comparison subjects or other comparison subjects included. To test the association of GM abnormalities with hallucination severity.	Structural MRI at 3 Tesla acquired with 1 mm slice thickness. Optimized VBM conducted with regression of hallucination severity to selected ROIs applying familywise error correction at $p < 0.05$. Structural covariance among these regions examined. Correlation tests were used.	Severity of hallucinations positively correlated with structural covariance among the left and right inferior frontal, left superior and medial temporal cortex, bilateral insula and right hippocampus. Correlations among the regions were not corrected for multiple testing. Multiple test correction for the VBM were applied but not for covariance among the regions.
13	Mitelman et al. (2006)	41 unmedicated SZ and 59 HC. To examine the correlations between the volumes of the pulvinar, centromedian, and mediodorsal nuclei of the thalamus and GM volumes of 39 cortical Brodmann's areas	1.5 Tesla structural MRI, 1.2 mm thickness slices. Examined parcellation of thalamus into pulvinar, centromedian nucleus and mediodorsal nuclei. Correlation with 39 Broadman's cortical areas was computed. Correlation tests were used. Multiple test corrections were applied uniformly as $p < 0.005$ although more tests overall were conducted.	Positive correlations between pulvinar and ipsilateral orbitofrontal and occipital cortices were found in controls but were weaker in SZ. Pulvinar volume correlation with DLPFC and temporal Brodmann's areas were significant in SZ but not in controls. Centromedian thalamic nucleus correlated positively with frontal regions in controls but not in SZ. Mediodorsal nucleus negatively correlated with area 36 in controls only
14	Mitelman et al. (2005a)	106 chronic SZ patients and 42 HC.	Examined the correlations between thalamic volumes and 39 cortical Broadman's areas (both gray and white volumes) corrected for total brain volume. Pearson correlation-based correlation matrices were built using these volumes.	SZ patients did not show correlation of thalamic GM volumes with prefrontal, medial temporal, posterior parietal, and occipital cortical regions while white matter volumes in rostral frontal and frontal eye field negatively correlated with thalamus. Poor outcome SZ group showed correlations between dorsal thalamus and ventral PFC compared to HC and good outcome SZ group. Controls showed positive correlations of dorsal thalamic volumes with frontal Brodmann's areas (8, 9, 10 and 46) and ventral thalamic volumes with areas 24 and 32. Medial temporal gray volumes negatively correlated with central and dorsal thalamus on the right. Parietal GM volumes positively correlated while occipital volumes negatively correlated with thalamus. WM volumes did not show correlations with thalamus except for negative correlation with the entorhinal cortex WM volume.
15	Mitelman et al. (2005b)	106 SZ and 42 HC. To examine correlations of frontal GM and WM volumes within each of the 11 Brodmann areas and with Brodmann areas of other cortical regions.	Examined correlations of frontal gray and white matter volumes within each of the 11 Brodmann's areas and with Brodmann areas other cortical regions. Multivariate Kullback test for correlation matrices was used to compare the correlation matrices of healthy controls with good prognosis and poor prognosis patients. Also used PCA as a second multivariate test for correlational differences Bivariate Pearson correlation tests were used for posthoc comparisons of within each hemisphere between relative gray and white matter volumes of the 39 cortical Brodmann's areas. A second PCA was conducted for each hemisphere.	HC showed significant positive correlations within the frontal region among adjacent areas for both gray and white matter volumes; ≈80% of correlations were positive especially for white matter volumes. Extensive positive correlations of frontal GM volume with medial temporal lobe structures, frontal with occipital GM volumes, and intrafrontal and frontal with temporal/occipital/parietal white matter volumes also reported. Compared to controls, patients showed correlations on the right frontal lobe but not on the left. Patients showed a pattern of correlations that reflected fronto-temporal pathology. Poor outcome patients showed reduction or absence of fronto-cingulate and frontotemporal region correlations.
16	Mitelman et al. (2005c)	106 SZ and 42 HC Goal was to examine the relationship of GM and WM of temporal lobe BAs with rest of the cortex. Another goal to examine if these relationships are correlated with outcome	Examined intercorrelations between gray and white volumes of the Brodmann's areas of the temporal lobe with rest of the cortex. Bivariate correlation tests. Multivariate Kullback test of correlations	Patients showed stronger significant frontotemporal positive correlations with weaker negative correlations compared to controls. Primary auditory cortex (areas 41 and 42) positively correlated with occipital, parietal, cingulate and posterior fronto-parietal areas.

(*continued on next page*)

Table 1 (*continued*)

	Authors	Study Sample and goals	Methods	Main findings
				Areas 21 and 22 correlated with cingulate. Temporal areas positively correlated with frontal and prefrontal regions in SZ. These correlations were not observed in HC. Poor outcome patients showed stronger correlations between medial temporal and primary visual cortex, and between the primary auditory and the DLPFC compared to good outcome SZ and HC.
17	Buchanan et al. (2004)	44 chronic SZ patients and 34 HC. To examine the association of regions within the heteromodal association cortex with SZ pathophysiology.	1.5 Tesla MRI at 1.5 mm slices were examined. Focused on examining heteromodal association cortex consisting of prefrontal, superior temporal, and inferior parietal cortices. Prefrontal region was parcellated into 4 subregions. Inferior parietal cortex was subdivided into angular gyrus and supramarginal gyrus. Used Pearson correlations by adjusting for all other volumes examined but not for ICV, age or sex.	Volumes of heteromodal association cortices did not show group differences. Superior PFC and orbital PFC significantly correlated in both HC and SZ. Controls showed significant correlation between orbital PFC and superior temporal gyrus volumes. SZ patients showed significant correlations between inferior PFC and angular gyrus volumes, and between supramarginal and angular gyri volumes. The correlation between the inferior PFC and angular gyrus volumes in SZ patients was significantly different from that observed in HC.
18	Wible et al. (2001)	17 chronic male schizophrenia subjects and 17 male healthy controls. This data was combined with their own previously published data on 15 schizophrenia patients (Wible et al., 1995).	1.5 Tesla MRI data at 1.5 mm slices examined. Hand drawn ROI measurements of frontal lobe and temporal regions on a preprocessed imaging data. Combined frontal lobe measures with previously published data on prefrontal region. Pearson correlation tests used to examine structural covariance	Positive correlations between prefrontal and posterior amygdala-hippocampal complex were found in patients but not in controls
19	Niznikiewicz et al. (2000)	15 male chronic SZ patients and 15 male HC. To examine the relationship of angular gyrus, supramarginal gyrus, prefrontal, and temporal regions with SZ, and to explore correlation with formal thought disorder, attention and working memory.	1.5 Tesla scanner data with 3 mm slices Pearson correlation tests for absolute measures of volumes and corrected for intracranial volume was implemented.	Significant correlations found between left and right inferior parietal lobule volumes in both SZ and HC, and between the left and right superior parietal gyrus, and between the left and right postcentral gyrus. Significant group differences in correlations noted for the left inferior parietal lobule and prefrontal structures with higher correlations for SZ patients. Formal thought disorder severity did not correlate with any of the volumes. Visual attention, visual memory and Trails A performance negatively correlated with reduced inferior parietal lobule volumes.
20	Wright et al. (1999)	27 multiplex SZ and 37 HC. To examine correlational structure in the supra-regional brain volumes.	1.5 Tesla scanner data with 1.5 mm slices were processed for GM density and ventricular-CSF density maps. GM maps were further divided into frontal-parietal, frontal-temporal, and frontal-basal ganglia components. Used singular value decomposition to obtain principal components of each matrix.	SZ patients showed globally decreased GM and globally increased ventricular-CSF measures. Patients also showed decreased prefrontal-temporal GM measures. The third, fourth and the fifth principal components (PCs) showed meaningful components. The third PC included bilateral frontal cortex, superior parietal lobule and precuneus. The fourth PC contained the frontal-temporal regions. The fifth PC comprised of the fronto-thalamic regions. The first PC (global gray and ventricular regions) suggested less GM and more ventricle contributions, and the fourth PC showed significantly reduced scores, in SZ than in HC.
21	Bullmore et al. (1998)	35 right-handed SZ and 35 HC. To identify abnormal correlation structure in imaging data.	1.5 Tesla data Correlation tests used	Most inter-regional correlations were positive in controls whereas patients showed near 0 or negative correlations. Positive correlations in controls were observed in the frontal lobe, dorsolateral and ventrolateral PFC, temporal lobe, superior temporal gyrus, parahippocampal gyrus, hippocampus, posterior and anterior cingulate gyrus.
22	Portas et al. (1998)	15 chronic male SZ and 15 male HC. Investigate thalamic volumes differences in schizophrenia	1.5 Tesla MRI data at 1.5 mm slices examined. Controlled for the volumes for ICV, and then partialled out SES and age Spearman correlation tests were used to examine structural covariance.	No differences in thalamic volumes between patients and controls. Observed significant negative correlations between left and right thalamus with left and right ventricles among SZ, but not among HC. Right hippocampus and right thalamus were correlated with each other among HC but not in SZ.
23				

(*continued on next page*)

Table 1 (*continued*)

	Authors	Study Sample and goals	Methods	Main findings
	Woodruff et al. (1997)	42 right-handed male SZ patients compared to 42 matched unaffected controls. To test correlations among brain regions, data were available for 36 SZ and 38 HC.	1.5 Tesla MRI data with 3 mm slices. Dissociation between frontal and temporal volumes were studied. Correlation tests used	Positive correlations ($r > 0.4$) were found in HC between bilaterally averaged regional measurements in frontal (e.g., DLPFC) and temporal lobes (STG, parahippocampal gyrus and hippocampus) along with positive correlations between anterior cingulate, temporal lobes and DLPFC, and between posterior cingulate and hippocampus. Patients showed lower correlations ($r < 0.4$) between temporal and frontal regions except between the dorsolateral and ventrolateral prefrontal cortices.
24	Wible et al. (1995)	15 chronic SZ and 15 HC Investigation of GM and WM differences in the prefrontal and temporal lobes.	1.5 Tesla MRI data at 1.5 mm slices examined. Hand drawn ROI measurements of PFC was obtained. Temporal lobe ROIs from the previous study (Shenton et al., 1992) were used. Pearson correlations were used to test the correlation among these regions.	No group differences observed between patients and controls in prefrontal cortical volumes. Prefrontal gray and white matter volumes correlated with volumes of anterior hippocampal-amygdala complex, anterior parahippocampal gyrus and anterior STG in SZ. HC showed significant positive correlations of the anterior hippocampal-amygdala complex and anterior parahippocampal gyrus with prefrontal white but not GM volume.
25	Breier et al. (1992)	44 medicated stable chronic SZ and 29 HC To examine volumetric differences in the prefrontal, temporal and caudate regions between SZ and HC, and to examine correlations among each other.	2-Tesla scanner operating at 1.5 T. 3 mm slices were examined. Landmark based ROI definitions used. Examined both GM and WM Partial correlations corrected for age and sex were used.	SZ patients showed smaller volumes of bilateral amygdala/ hippocampal complex; right prefrontal GM was not reduced. Right prefrontal WM was reduced and correlated with amygdala/hippocampal volumes; left prefrontal WM did not correlate. HC did not show such correlations.
26	Shenton et al. (1992)	15 chronic SZ and 15 HC To examine case-control differences in volumes and correlations among these regional volumes	1.5 Tesla MRI data with 3 mm slices. Regions were identified using combined automated and manual segmentation and hand drawn ROIs. ICV-corrected volumes were used in testing the correlations among the regions.	SZ patients showed left temporal horn volume significantly negatively correlated with left parahippocampal gyrus. Left parahippocampal gyrus positively correlated with left posterior hippocampus. Left anterior superior temporal gyrus correlated with left anterior amygdala-hippocampal complex. HC did not show correlations among these regions. Probably the first MRI study that examined the correlation among selected structures

Abbreviations used: ACC, Anterior Cingulate Cortex; BD, Bipolar disorder; CAT, Computational Anatomy Toolbox; DLPFC, Dorsolateral Prefrontal Cortex; DMN, Default Mode Network; FDR. False Discovery Rate; GIFT, Group ICA for fMRI Toolbox; GLM, General Linear Model; GM: Gray Matter; HC, Healthy Controls; ICA, Independent Component Analysis; IQ, Intelligence Quotient; HC, Healthy Controls; MDD, Major Depressive Disorder; MPFC, Medial Prefrontal Cortex; MTG, Middle Temporal Gyrus; PANSS, Positive and Negative Symptoms Scale; PFC, Prefrontal cortex; ROI, Region-of-Interest; SBM, Source based morphometry; SCN, Structural Covariance Network; SPM, Statistical Parametric Mapping; STG, Superior Temporal Gyrus; SZ, Schizophrenia; ToM, Theory of Mind; VBM, Voxel-based morphometry.

fronto-temporal regions among controls but negative or no correlations in patients. Averaging regional volumes from both hemispheres on a larger sample, Woodruff et al. (1997) reported stronger correlations in controls than in patients for the fronto-temporal regions except between the dorsolateral PFC (DLPFC) and ventrolateral PFC.

Later studies reported correlation of thalamus with ventricles in patients but with hippocampus in controls (Portas et al., 1998), higher fronto-parietal correlations in patients (Niznikiewicz et al., 2000), and different patterns of correlations in patients and controls in the hetero-modal association cortices (Buchanan et al., 2004). Chen et al. (2014b) reported differences in covariance among insula, amygdala and parietal regions between patients and controls in a network of regions selected based on metanalysis.

Multivariate statistical methods were also used to examine SCN of selected regions. Corradi-Dell'Acqua et al. (2012) used PLS approach to structural equation modeling (SEM). SEM analyzes structural relationship between real variables and latent constructs to build models of processes that would give rise to the observed data. They found co-efficients of paths connecting the thalamus to the anterior insula, and the DLPFC to the amygdala were larger, while path from the entorhinal cortex to the DLPFC was smaller in patients compared to controls demonstrating dysconnectivity among these regions. However, details on statistical analysis were not provided (Table 3).

3.2.2. *Whole brain parcellation-based SCN*

Some SCN studies examined structural covariance either within regional network specialization, seed-based SCN or regions regulating cognitive processing using multivariate and correlational approaches.

3.2.2.1. Whole-brain SCN studies examining regional network specialization. When inter-regional and interlobar covariance was examined separately, patients showed both stronger and weaker coupling. Stronger coupling between the frontal lobes, frontal-limbic and temporal-subcortical but weaker frontal-subcortical coupling was observed in patients. Two subnetworks were identified. Greater coupling between limbic to frontal, and limbic to parieto-temporal regions weaker coupling between frontal-parieto-occipital and among medial temporal regions was noted Inter-regional couplings within the lobes showed pairwise correlations of regions spread out in every lobe/region in both patients and controls (Collin et al., 2013).

Whole thalamic GM did not correlate with prefrontal and medial temporal (Mitelman et al., 2005a) but pulvinar nucleus volume negatively correlated with prefrontal and temporal regions in patients. Posterior parietal, and occipital regions while rostral frontal and frontal eye field WM volumes negatively correlated with thalamus in patients (Mitelman et al., 2006). Healthy controls showed different pattern where GM volumes but not most WM regions showed correlations (Mitelman et al., 2005a) and centromedian nucleus positively correlated

Table 2
Cource-based morphometry studies in schizophrenia.

Source-Based Morphometry				
1	Penzel et al. (2021)	102 patients, ages 15–40, with Recent Onset Psychosis, and cannabis use within 2 weeks of psychosis onset, and/or lifetime cannabis abuse or dependence. The main goal is to determine if cannabis use patterns affect structural morphology and positive psychotic symptoms.	Structural MRI data was acquired from the Personalized Prognostic Tools for Early Psychosis Management (PRONIA) and Cannabis Induced Psychosis (CIP) projects. Conducted source-based morphometry (SBM) and voxel-based morphometry (VBM) were used to compare GM components in recent onset psychosis patients with cannabis use.	Earlier cannabis use (by age) was associated with more severe positive symptoms as well as onset of first attenuated psychotic symptoms. Using SBM, a GM component was identified representing the cerebellum which was associated with earlier cannabis use. This component was negatively correlated with another component which consisted of superior temporal, precentral, frontal and parahippocampal gyrus and insula, indicating that reductions in these areas were associated with increases in cerebellar GM volume. VBM analysis showed no significant findings, but authors state that the VBM findings trended in line with the SBM findings.
2	Quide et al. (2021)	166 participants (55 SZ cases, 52 BD cases, 59 HC). Goal was to examine the direct and indirect relationships between childhood trauma severity, systemic inflammation, and patterns of gray matter covariance among brain regions.	T1-weighted anatomical scans with slice thickness of 0.9 mm collected on 3 T scanner. Peripheral blood from all participants were assayed for inflammatory markers and a composite score representing systemic inflammation for each subject was calculated by summing the z-scores of each marker levels. Using the individual pre-processed GM images, an ICA was computed using the Infomax algorithm within the GIFT. The PROCESS macro (v3.4) for SPSS was used for a series of moderated moderation analyses. Group (HC, BD, SZ) was entered as the moderators of the association between each GM IC and systemic inflammation by severity of childhood trauma exposure.	Striatum showed higher volume with greater inflammation regardless of the diagnosis. Systemic inflammation was associated with *decreased* gray matter covariance in posterior cingulate cortex/ precuneus, parietal and postcentral gyrus (which are considered "social brain") and *increased* gray matter covariance in the middle temporal gray matter in healthy individuals exposed to high levels of trauma, and with low levels of trauma in SZ but not in BD cases. Childhood trauma did not mediate inflammation of brain morphology in BD.
3	Rodrigue et al. (2020)	SBM was conducted on 20,306 individuals from the UK Biobank sample. Goal was to examine whether SBM generated networks can be used as phenotypes for genetic analysis by estimating heritability, understanding genetic architecture including pleiotropy, and their genetic relationship with SZ, BD and MDD.	MRI data acquired using 1 of 3 dedicated 3 T scanners (Siemens Skyra, VB13). Preprocessed using FSL and customized VBM under FSL. GIFT toolbox was used to implement ICA using infomax algorithm with a model order of 25. Imputed genotypes provided by the Biobank was used for genetic analyses.	SBM identified 25 spatially distinct components; 7 networks were assigned to a cognitive control module, 6 to a default mode module, 5 networks to a sensory module, and 7 networks to a cerebellar module. Significant but modest heritability was observed for many networks. Some networks were highly polygenic. 27 linkage disequilibrium-independent variants were associated with one or more networks and other phenotypes. Seven nominally significant associations with SZ, BD and MDD were found; of which the association of default mode network component 10 with SZ survived FDR corrected significance.
4	DeRamus et al. (2020)	167 SZ and 159 controls were used. To develop source-based laterality and apply to SZ and HC	First, a simulation was used to demonstrate robustness of the method. Next, the method was	Thirty components were selected; none of them were identified as artifacts. Ten regression models significant after

(*continued on next page*)

Table 2 (*continued*)

Source-Based Morphometry				
			applied to 300 simulated subtraction maps. Finally real data of SZ and HC were used. Data were from 7 imaging centers across the MIND research network.	FDR correction at 5%. Four of these components were related to diagnosis of SZ. Post hoc Wilcoxon rank-sum tests91 identified significantly greater cerebellar component weights in HC participants compared to SZ, but significantly reduced weights in HC participants compared SZ participants in STG components, STG/MTG/ postcentral components and MTG components.
5	Rahaman et al. (2020)	382 structural MRIs from SZ patients were included – no HC data is used. Goal was to test the performance of a clustering algorithm to sub-classify SZ subjects, and test on a simulation data set.	Used a data-mining technique known as "biclustering" to determine if SBM results from neuroimaging data can be used to sub-classify psychiatric subjects.	The proposed biclustering was more "robust" than existing approaches. The authors suggest using the clustering method to leverage SBM analysis for the detection and measurement of homogeneity in imaging data. The study identified two components related to positive (inferior temporal gyrus) and negative (brain stem) negative symptoms. Since the authors do not make use of HC data, neuropsychiatric conclusions from the clustering analysis are limited; however, clustering on the 382 real-world structural SZ MRI data reveals that SBM-based clustering significantly corresponds to symptomology.
6	Wolf et al. (2020)	22 SZ spectrum disorder (SSD) patients with scores >4 on Simpson-Angus scale (SAS) and 22 SSD patients with SSA scores <4.	3D MPRAGE MRI data and 6-min resting state fMRI acquired on a 3 Tesla scanner and the data were processed using VBM first	Five IC pairs were significantly correlated between the modalities. Groupwise comparison showed one IC in each modality was

Table 2 (*continued*)

Source-Based Morphometry				
		Goals were to examine modality-specific and transmodal fronto-parietal and frontostriatal networks in SSD with SAS scores <4 and > 4, and to examine dimensions of parkinsonian symptoms associated with the networks.	followed by parallel ICA.	significant. The structural IC comprised of MFG, IFG, ACC, thalamus, precentral gyrus, and cerebellar regions (frontothalamic/ cerebellar IC). Functional IC had cuneus and lingual gyrus (cortical sensorimotor IC). Fronto-thalamic/ cerebellar IC correlated with glabella-salivation score. Cortical sensorimotor IC correlated with tremor and glabella-salivation score.
7	Sorella et al. (2019)	46 SZ, 46 BD, and 66 HC. Used SBM to test the hypothesis that a continuum of "psychotic core" exists between SZ and BD. Also hypothesized that there will be differential compromise on the affective and cognitive cores	3 T structural MRI were acquired on Siemens Trio scanner. Illness-associated deficits are measured using cognitive, affective, and clinical tests. SPM-12 and CAT-12 were used to process T1W images. Subject-level results of SBM implemented using the GIFT toolbox and then compared between groups. SBM component values across participants were tested for correlations between psychological and morphometric results.	Authors found significant reductions in components representing large cortical areas in the BD and SZ groups compared to HC. Comparing BD to SZ revealed reductions in the component corresponding with the superior and middle frontal gyrus, superior and inferior parietal lobule and, the precuneus in SZ compared to BD. Cognitive testing indicated that the SZ group had more severe cognitive deficits, whereas the BD group had lower affective profiles. Authors show evidence that these cognitive differences correspond to SBM component strength by group, supporting their initial hypothesis.
8	Li et al. (2019)	62 first-episode and drug-naive SZ patients. Goal to investigate the spatial pattern of progressive gray matter changes that predict the symptomatic treatment	3 T scanner used to collect T1 images with 1 mm slice thickness at baseline and 1 year. SBM analysis was carried out using Group ICA Toolbox using standard	The GM volume of ACC, anterior insula, STG, MTG, DLPFC, precuneus, and inferior parietal lobule decreases over a 1-year period after commencing treatment for first-episode

(*continued on next page*)

Table 2 (*continued*)

Source-Based Morphometry				
		response after 1-year follow-up.	procedures with the number of components set at 30. Performed a series of linear regression analyses with loading scores of GMV components as the dependent variable. Symptom scores at the baseline were included as predictors.	schizophrenia. At the onset of first episode, the presence of lower GM volume in bilateral inferior frontal gyrus and anterior insula predicted lack of a linear improvement in positive and disorganization symptoms despite antipsychotic treatment over 1 year. The presence of more severe symptoms during the first episode of psychosis does not indicate more pronounced gray matter reduction by 1 year.
9	Quide et al. (2018)	214 Caucasian SZ cases and 94 Caucasian HC Goal to examine the effects of variation of the rs1344706 polymorphism on GM integrity.	High-resolution T1 -weighted structural MRI scans collected on a 1.5 T scanner with a voxel size of $0.98 \times 0.98 \times 1.0\ mm^3$. Scans were pre-processed using CAT12 routine for VBM and SBM. ICA was conducted on pre-processed GM images using the Infomax algorithm within the GIFT v4.0a toolbox. The number of components were estimated using the 'minimum description length' criteria. Maps for each significant component were overlaid on a MNI template, and stereotaxic coordinates from clusters above a $z > 2.5$ threshold were obtained using the Talairach Daemon database. Genotyping for rs1344706 was performed on	SZ showed significantly reduced GM volume relative to HC in two large clusters including: (1) the right rectus gyrus, medial orbital gyrus, medial frontal gyrus and left and right ACC; and (2) the left fusiform gyrus, occipital fusiform gyrus, inferior temporal gyrus, exterior cerebellum, and inferior occipital gyrus. There was no significant effect of rs1344706 genotype on any voxel. SZ group showed lower GM thickness in a cluster including the left lateral orbitofrontal gyrus, in a cluster encompassing the left inferior temporal and fusiform gyri and a cluster in the right pars opercularis and precentral gyri. No significant genotype effect on thickness. From the 16 derived components form SBM there was a significant effect of diagnosis on components 5, 9,

Table 2 (*continued*)

Source-Based Morphometry				
			Illumina's Infinium Psych Array Bead Chip. To identify SBM-derived ICA components associated with SZ, a hierarchical logistic regression was performed. Bonferroni correction was applied to account for the number of components significantly associated with a diagnosis.	and 12. Component 5 (C5) comprised positively correlated voxels encompassing the left and right lentiform nuclei, caudate, and insula, and negatively correlated right insula voxels. Component 9 (C9) comprised negatively correlated voxels within the left and right middle and medial frontal gyri, anterior cingulate and cingulate gyri, superior frontal and precentral gyri. Component 12 (C12) comprised negatively correlated voxels in regions including the bilateral insulae, inferior, middle, and medial frontal gyri, STG, parahippocampal gyri, inferior parietal lobules, subcallosal gyri, postcentral gyri as well as left transverse temporal gyrus, and left middle frontal gyrus. No influence of rs1344706 on GM (volume and thickness) integrity in SZ. Limitations of the present study include the possible effects of antipsychotic medication, small HC sample, small n of homozygotes in the HC, uneven distribution of age and sex across studies. Epistatic effects of this gene variant with others may have synergistically affected brain morphology during brain development.
10	Gupta et al. (2017)	382 SZ patients. No HC Goal was to evaluate the relationship	1.5 and 3 Tesla data from 3 independent studies (one being	3 subtypes were obtained: Subtypes S_1 (65 subjects weighted on only I-STG-IFG

(*continued on next page*)

Table 2 (*continued*)

Source-Based Morphometry				
		between symptoms and SBM loadings in subsets of SZ patients obtained through loadings from 2 components comprising of insula/STG /inferior frontal gyrus (I-STG-IFG component) and superior/ medial/middle frontal gyrus (SFG-MiFG-MFG component) which had large effect size and showed diagnostic differences in their previous work.	multisite) from nine scanning sites that had PANSS data. Inter-scanner reliability data were not available. Regressed out the site variable on PANSS scores. Biclustered ICA (Bi-ICA) was implemented to identify subtypes. Using the subtype-specific components, group information guided-ICA (GIG-ICA) was implemented. Structural network connectivity was measured using correlations between loadings from two ICs.	component), S_2 (62 subjects highly weighted on only the SFG-MiFG-MFG component), and an intersecting group S_{inter} (53 subjects highly weighted on both components). PANSS positive scores in subtypes S_1 (mean = 13.68) and S_2 (mean = 16.74) showed a significant difference (Wilcoxon rank sum test = 3954 ($n_1 = 65$, $n_2 = 62$, $p = 0.006$). Few subjects in subtype S_2 captured high PANSS positive scores. No significant differences in PANSS negative scores and PANSS general scores were observed between S_1 and S_2. Structural network connectivity between the three components showed different strengths of connectivity. Since patients were on medications, severity of symptoms on PANSS are very likely influenced by medication response. Medication data were not available on all patients. Not including HC precludes comparison of the subtypes to "non-disease" brain.
11	Wolf et al. (2016)	42 Participants (21 ECT-naive patients (12MDD, 9SZ), 21 healthy controls) Investigate the effects of ECT on brain structure of patients with treatment resistant MDD and SZ.	T1-weighted image acquired on 3 T MRI with resolution of $1mm^3$. Initial scan with 5 days of first ECT session, post-ECT scan acquired 6–8 days after last stimulation. A voxel-based morphometry (VBM)analysis was computed using Christian	SZ patients showed 5 networks (precuneus, bilateral thalamus, medial temporal lobe, left DLFPC/ ACC and bilateral cerebellum were different before ECTs. SZ patients showed an improvement in 2 of the 5 networks after ECT. There was a significant negative

Table 2 (*continued*)

Source-Based Morphometry				
			Gaser's VBM toolbox running with in the Statistical Parametric Mapping software package version 8 (SPM8). Patient data were processed according to longitudinal processing pipeline. Employed the SBM algorithm as implemented in the "Group ICA for fMRI Toolbox" (GIFT) ECT-effects on structural networks in MDD and SZ were analyzed offline using the Statistica software package.	association between PANSS total score differences and the left DLPFC network strength change but associations between sub scores were not significant. Identified 4 structural networks (ACC/ medial PFC, bilateral thalamus, medial temporal lobe, left cerebellar/ precuneus) showed significant differences between healthy controls and MDD patients. MDD patients showed an increase in structural network strength in 2 of the 4 networks (ACC/ medial PFC, and medial temporal lobe) after ECT but nether were associated with clinical improvements. For completeness tested for ECT-related changes in networks not significantly difference between patients and healthy control and found no significant findings.
12	Sprooten et al. (2015)	Investigated genetic influence on SZ-associated SBM components in 887 individuals from 69 pedigrees with Mexican American ancestry. Families ranged from 1 to 90 members, aged 18–85 years.	T1w images collected at 3 T, voxel dimensions unspecified. SBM was used to identify an insula-MPFC component. A gene linkage analysis was performed to identify heritability and gene locus associated with the GM component.	The study reported significantly different weights on the insula–MPFC component in SZ patients versus HC, suggesting that the SBM-derived insula-MPFC component is associated with SZ. The SZ-associated component was significantly heritable. The linkage analysis revealed 12q24 to be the significantly associated with the insular-MPFC GM component.
13				

(*continued on next page*)

Table 2 (*continued*)

Source-Based Morphometry				
	Palaniyappan et al. (2015)	19 SZ patients and 20 HC Goal was to determine if the presence of structural alterations across distributed anatomical 'subsystems' in relation to the variations in severity of persistent formal thought disorder in clinically stable SZ patients.	T1 weighted images acquired on a 7 T scanner with 0.6 mm isotropic resolution. SBM analysis was carried out using Group ICA Toolbox as using standard procedures. The number of independent components was estimated using minimum description length criteria. Statistical tests were implemented on SPSS v 21.0. A patient vs. controls comparison on the 8 spatial components was performed using MANOVA followed by Bonferroni corrected univariate tests.	A significant proportion of the variance in negative formal thought disorder was explained by morphometric variations in the distributed brain regions (especially frontotemporal cortex, striatum, insula, anterior and posterior cingulate cortex and precuneus) Both increased and decreased gray matter volumes were noted in association with formal thought disorder.
14	Gupta et al. (2015)	784 patients with SZ and 936 HC from 23 sites	1.5 and 3 Tesla MRI data. Preprocessing was done in SPM5. Performed both SBM and VBM analyses on GM concentration images.	Seven of the identified SBM components showed less GM concentration in SZ while 2 components had increased GM concentration in SZ. The largest GMC difference between diagnostic groups in the network included the superior temporal gyrus, inferior frontal gyrus, and insula. No spatial patterns of GM concentration difference were related to the measures of symptom severity.
15	Chen et al. (2014a)	1460 HC collected from multiple scan site were used to test scanner-effect. A second sample with 110 SZ patients and 124 HC was used to demonstrate how SBM can remove scanner-effects.	Data was collected at one of 4 scan sites with either 1.5 or 3 Tesla field strength. Voxel dimensions varied. Introduced an approach to use SBM to remove scanner-derived artifact components. Compares this approach to traditional GLM approaches.	SBM analysis of the 1460 HC revealed scanner effects in the brainstem and thalamus that were associated with magnetic field strength-inversion time and RF-receiving coil. In the smaller two-group sample, SBM-corrected scanner artifacts led to higher significance of SZ-HC differences than using GLM approach to remove scanner effects. The component that best discriminated the patient and control group corresponded to the frontal temporal network.
16	Kubera et al. (2014)	20 right-handed paranoid SZ and 14 HC. 10 SZ were classified as chronic with persistent auditory verbal hallucinations (AVH).	3 Tesla MRI data with 1 mm slices. VBM toolbox within SPM8 was used for the segmentation. ICA was computed using an Infomax algorithm. Calculated Spearman correlations between brain volume and AVH-specific measures.	In the entire sample of SZ patients, a pattern of predominantly lower lateral prefrontal GM volume independent of AVH persistence was found. Patients with chronic, treatment-resistant symptoms additionally showed a pattern of predominantly lower lateral medial frontal and lateral temporal GM loss which differentiated them from both HC and SZ patients who did not have persistent AVH. The pattern of lower medial frontal and lateral temporal GMV in persistent AVH patients is significantly associated with characteristics of AVH, such as symptom duration, location, frequency, and intensity.
17	Turner et al. (2012)	Two independent datasets were examined, both consisting of schizophrenia patients: 209 patients versus 208 controls; 102 patients versus 96 controls. VBM and SBM methods were	Both 1.5 and 3.0 Tesla MRIs were used; voxel and slice thicknesses varied. Clinical correlates and heritability of SBM group-difference results were examined.	In both datasets, patients showed significant GM reductions in cortical frontal, temporal, and insular lobe by VBM analysis. SBM analysis extracted 24 components, 4 of which had significantly lower gray matter concentrations in patients. Two

(*continued on next page*)

Table 2 (*continued*)

Source-Based Morphometry				
		and compared to clinical data.		components were determined to be related to familial heritability. These components together represented the medial frontal, insular, inferior frontal, temporal lobes, and posterior occipital lobe. Authors suggest SBM can detect heritable endophenotypes of schizophrenia.
18	Xu et al. (2012)	121 patients with SZ and 120 HC. Goal was to identify structural networks showing group differences and common inter-subject covariation.	SBM was performed on the angle/power image set using the GIFT toolbox. This SBM approach consisted of three steps: independent component analysis (ICA), statistical analysis, and visualization	Results indicated that white matter concentration was higher and GM concentration was lower in the thalamus in SZ. Structural angle feature identified the most sources showing group differences. The power angle identified an important previously identified network in which both groups have larger GM values. Structural angle and power images revealed several findings in SZ that were not identified by standard gray or white matter analyses and demonstrates the usefulness of angle and power joint gray and white matter assessment.
19	Kasparek et al. (2010)	49 first episode SZ compared to 127 HC. Hypothesized that SBM would be better at detecting group differences than VBM.	1.5 Tesla with voxel size 1.17 × 0.48 × 0.48 mm. SZ and HC were compared by both VBM and SBM methods to determine if SBM improves group difference detection over VBM.	VBM was unable to detect any group difference at either the voxel or cluster level. SBM detected group differences in 3 out of 13 non-artifact independent components supporting the authors' hypothesis. GM volume reductions associated with first-episode SZ found in the prefrontal, temporal, and cerebellar regions. The parietal and occipital cortex both were found to have GM volume increases in SZ.
20	Xu et al. (2009a)	120 chronic SZ patients and 120 HC. Identify linked gray and white matter regions which differ between groups using joint-SBM.	1.5 Tesla structural MRI whole brain images preprocessed using SPM5. Separate gray and white matter images were extracted. GM images were processed using the spatial ICA implemented on GIFT toolbox using the Infomax neural net program. *t*-tests on the mixing matrix reveal significant joint source differences. Visualization step used the source matrix from JICA to create joint source map to identify regions.	Five "source networks" were identified consisting of bilateral temporal, thalamus, basal ganglia, parietal, and frontal/temporal areas. Each of these sources included many other regions covarying, e.g., source 1 that had STG as the source consisted of many other regions such as ACC, medial, middle, and superior frontal gyrus along with other subcortical regions. Sex did not significantly associate with these 5 sources, but age correlated with source 1 and 4. In all these sources, HC had more GM than SZ patients. All regions found in VBM were found by the SBM, but SBM identified more regions.
21	Xu et al. (2009b)	120 chronic SZ patients and 120 HC. To use SBM to examine the association of GM components with SZ.	1.5 Tesla structural MRI data with 1.5 mm slices. VBM toolbox in SPM5 for preprocessing. Joint ICA using infomax algorithm on gray and white matter images using both SZ and HC.	Four significant joint sources were found: temporal-corpus callosum, occipital/frontal-inferior fronto-occipital tract (in these two sources, loading parameters were lower in patients), frontal/parietal/occipital/temporal-superior longitudinal fasciculus, parietal/frontal-thalamus (loading parameters for these were higher in patients). Four were selected after visual inspection of 7 where 3 of the ICs had artifacts. Joint sources reveal linked gray and white matter regions that have a significant difference between groups.

(*continued on next page*)

Table 2 (*continued*)

Source-Based Morphometry				
				Joint sources were correlated with age. Gray and white matter regions have the same contribution to inter-subject covariation. Controls tend to have more gray matter and patients have more white matter.

Abbreviations used: ACC, Anterior Cingulate Cortex; BD, Bipolar disorder; CAT, Computational Anatomy Toolbox; DLPFC, Dorsolateral Prefrontal Cortex; DMN, Default Mode Network; FDR. False Discovery Rate; GIFT, Group ICA for fMRI Toolbox; GLM, General Linear Model; GM: Gray Matter; HC, Healthy Controls; ICA, Independent Component Analysis; IQ, Intelligence Quotient; HC, Healthy Controls; MDD, Major Depressive Disorder; MPFC, Medial Prefrontal Cortex; MTG, Middle Temporal Gyrus; PANSS, Positive and Negative Symptoms Scale; PFC, Prefrontal cortex; ROI, Region-of-Interest; SBM, Source based morphometry; SCN, Structural Covariance Network; SPM, Statistical Parametric Mapping; STG, Superior Temporal Gyrus; SZ, Schizophrenia; ToM, Theory of Mind; VBM, Voxel-based morphometry.

with frontal regions (Mitelman et al., 2006). also reported several findings suggestive of fronto-temporal dysconnectivity in patients compared to controls (Mitelman et al., 2005b; Mitelman et al., 2005c).

Hierarchical brain organization showed global and selected supra-regional covariance structure alterations in schizophrenia. Suprare-gional anatomy was defined by authors as structural changes in multiple brain areas as opposed to global measures and regional volume changes (Wright et al., 1999). Using singular value decomposition to extract PCs of GM volumes to identify altered brain organization at these levels, they showed that the global (GM-ventricular system) and supra-regional (fronto-temporal system) were orthogonal to each other and suggested that two different processes may underlie this pattern. The assumption was that the supraregional alterations reflect shared neuro-developmental influences.

3.2.2.2. Seed-based SCNs. Six studies examined the covariation of one or more regions selected as "seed(s)" based on study-specific hypothesis to examine covariation with morphometry of other regions using different approaches. While Clos et al. (2014), Abbs et al. (2011) and Spreng et al. (2019) examined volumes, others examined cortical thickness. Buchy et al. (2017) and Kuang et al. (2017) used the Pearson correlation to build the network and used the Mapping Anatomical Correlation Across Cerebral Cortex (MACACC) program which was designed to test seed-based anatomical covariance and compare across groups (Lerch et al., 2006). Moberget et al. (2018) used a meta-analytic approach while Clos et al. (2014) used SCN, resting fMRI and meta-analytic connectivity modeling. Abbs et al. (2011) examined gender differences in covariation among regions showing sexual dimorphism and also involved in verbal memory regulation in schizophrenia. Spreng et al. (2019) used PLS regression in a seed-based SCN within the networks that regulate cognitive domains to determine consistent SCN network alterations and the relationship of covariance network score with psychopathology. Given different methods, seed-regions and morphometric measures used, the results also differed.

The ventrolateral PFC seeded SCN did not show case-control differences (Kuang et al., 2017). Right somatosensory cortex and bilateral fusiform face area-seeded SCN showed higher covariance in controls than patients (Buchy et al., 2017). Cerebellum-seeded analysis showed positive correlations of cerebellar volume with cortical thickness of

Table 3
Multivariate statistical approaches to investigate structural covariance networks in schizophrenia.

Multivariate statistical approaches				
Partial Least SQ				
1	Spreng et al. (2019)	90 chronic SZ discovery and 90 demographically matched HC; 71 chronic SZ replication sample and 74 demographically matched HC. To use a novel seed-based approach using multivariate statistical approach to identify large scale SCNs.	Seed-based partial least square multivariate approach Examination of networks involved in salience, default, motor, visual, fronto-parietal, and dorsal attention based on functional architecture. Main goal was to test whether SCNs can show robust and replicable network-level alterations in patients compared to controls. For each participant, a composite structural covariance network score was calculated that indexed a network pattern identified by the latent variables and integrity of individual's network integrity. This score is mathematically expressed as the dot product of GM voxel value in each participant's normalized segmented image and the corresponding voxel weight in the spatial pattern derived from the thresholded PLS group result image.	Across two SZ samples, reliable and robust reductions in structural integrity of the fronto-parietal control and salience networks were found but not in the default, dorsal attention, motor, and sensory networks. Structural covariance scores did not correlate with symptoms measured on PANSS, but patients showed across-subject relationship for all structural networks consistently. Certain patterns emerged suggesting that the structural covariance score may be a trait-like measure with strong-across network relationship where same subjects might have low/high network covariance across networks.
Lasso-like regression				
2	Lefort-Besnard et al. (2018)	Resting state and structural MRI data from 5 different samples acquired in Europe and USA (241 SZ and 241 HC). To examine interactions between structural and functional networks involving DMN subnodes to gain insights into schizophrenia psychopathology.	Focused on three networks, namely the default mode, salience, and the dorsal attention networks. Examined the structural network concordance with the functional networks and, also the across network covariation. DMN subnodes included the	Using precision matrix (sparse inverse covariance estimates), authors report functional covariation between the right and the left temporo-parietal junction of the DMN to be significantly different between the HC and SZ whereas

(*continued on next page*)

Table 3 (*continued*)

Multivariate statistical approaches				
			dorsomedial PFC, primary motor cortex and temporo-parietal junction. DMN subnodes were supplemented by nodes of salience and dorsal attention networks.	the temporo-parietal junction and primary motor cortex showed structural covariation. Functional intra-network covariance was noted in the anterior temporo-parietal junction followed by dorsomedial PFC showing the highest number of disrupted functional connections in the default mode network. In the dorsal attention network, the left inferior parietal sulcus showed highest number of edges with significant disruption in SZ. In the salience network, SZ subjects showed disruption in the mid-cingulate cortex. Default mode network subnodes in the precuneus and the rostro-dorsal dorsomedial prefrontal cortex are the target regions with highest structural disturbances in SZ.
Machine learning model				
3	Castro et al. (2014)	110 SZ and 124 HC Components that have consistent contribution to the classification model and are less sensitive to inter-subject and inter-site variability.	1.5 or 3 Tesla MRI data with 1.5 mm slices. SPM5 was used to segment the images using unified segmentation. Used a machine learning approach based on resampling techniques to find consistent patterns of GM concentration differences. Consistent regions detected using SBM. Separated the brain into four components.	Multivariate analysis performed by Bagging SVM is capable of detecting relevant components that would be rendered irrelevant to schizophrenia based on univariate tests. It may be possible to replicate these results on multiple datasets. Three out of the four components showed an increase in GM concentration in HC when compared to SZ.
Structural Equation Modeling				
4	Corradi-Dell'Acqua et al. (2012)	68 chronic SZ patients and 77 matched HC Goals were to extend observations of frontal and mediotemporal region alterations by including thalamus and insula.	1.5 Tesla MRI data with 1.5 mm slices were examined for volumetric correlations among 5 ROIs: DLPFC, anterior insula, amygdala, thalamus, and entorhinal cortex.	Right anterior insula and DLPFC showed volume changes. Coefficient of the path connecting thalamus to anterior insula, DLPFC to amygdala was larger in patients than in controls. Coefficient of the path connecting entorhinal to DLFPC was smaller in patients than in controls
5	Liu et al. (2021)	Used 7 datasets: Initial dataset: 107 drug-naive first-episode SZ (FES) and 71 HC. Validation dataset #1: 44 drug-naive FES patients, 47 HC. Validation dataset #2: 166 drug-naive FES patients, 58 HC. Chronic dataset #1: 124 SZ patients, 132 HC. Chronic dataset #2: 67 SZ patients and 74 HC from the COBRE. Chronic dataset #3: 103 SZ patients and 89 HC from MCIC. A CHR dataset: 99 high-risk individuals, and 97 HC. Goals were to use normative models in stratifying individual patients and to externally validate normative models with symptoms and genotypes	Scan data obtained on either 3 T or 1.5 T scanners. VBM and CAT12 were used for initial processing AAL2 atlas was used for parcellation. Used the normative model that was developed in bioinformatics to construct individual-specific gene expression networks. Group level SCN of HC was first built after which one patient was added to create perturbation network. Perturbation networks were developed for each patient. From the *Z*-scores, individual differential SCNs were built. The three chronic and one CHR datasets were used to explore the stability of our results across different disease stages.	SZ patients were highly heterogenous in their SCNs. Despite high degree of heterogeneity, hippocampus and bilateral putamen/globus pallidus edges grouped patients into two opposing covariance patterns. Among the 4317 edges about 1/3rd edges were significantly different, and only about 28% of these were shared by at least 2 patients. Altered edges correlated with higher hallucinatory scores. Comparison of group level SCN with the IDSCNs showed that the accumulated differences in each patient contributed more strongly. Five variants of 4 genes were associated with edges of the hippocampus and putamen. CHR subjects showed similar group differences as the patients and two subtypes were present

(*continued on next page*)

Table 3 (*continued*)

Multivariate statistical approaches				
				even before the onset of the illness.
Granger causality				
6	Jiang et al. (2018)	97 SZ and 126 HC examined To assess causal relationship of structural alterations among the brain regions Patients were grouped into duration of illness of 0–10 year (Stage 1), 11–20 years (Stage 2) and > 20 years (Stage 3) 5-year interval staging was also used that had 6 groups	3 Tesla MRI data acquired at 1 mm thickness was processed using CAT12 in SPM12. Used Granger causality where morphometric data were ranked according to progression. The method was called causal SCN (CaSCN) to understand the progressive alterations of structural brain network throughout the duration of illness. GM volume data of patients sequenced according to the ranks of the SZ duration from low to high that is analogous to time-series information. This pseudo-time series was used to apply Granger Causality to construct seed based CaSCN. Positive Granger Causality value indicated that the same GM volume alteration in the regions lagged the seed atrophy suggesting that the reduction was driven by the seed; negative value suggested compensatory effect.	SZ showed reduced volumes in the thalamus, basal ganglia, frontal lobe, insula, pre- and postcentral gyrus, bilateral temporal gyrus, occipital cortex, and cerebellum with no regions showing increased volume. Duration of illness negatively correlated with volumes of regions. In stage 1, only thalamus volume was reduced. In stage 2, thalamus + prefrontal, insula and sensorimotor cortex were reduced. In stage 3, in addition to these, occipital, temporal and cerebellum showed reductions. CaSCN analysis that used thalamus as the seed showed positive Granger Causality value to the frontal, cingulate, insula, sensorimotor and other cortices. Authors suggest that thalamus may be a hub of brain regions showing volume reductions, which spreads to other regions

Abbreviations used: ACC, Anterior Cingulate Cortex; BD, Bipolar disorder; CAT, Computational Anatomy Toolbox; DLPFC, Dorsolateral Prefrontal Cortex; DMN, Default Mode Network; FDR. False Discovery Rate; GIFT, Group ICA for fMRI Toolbox; GLM, General Linear Model; GM: Gray Matter; HC, Healthy Controls; ICA, Independent Component Analysis; IQ, Intelligence Quotient; HC, Healthy Controls; MDD, Major Depressive Disorder; MPFC, Medial Prefrontal Cortex; MTG, Middle Temporal Gyrus; PANSS, Positive and Negative Symptoms Scale; PFC, Prefrontal cortex; ROI, Region-of-Interest; SBM, Source based morphometry; SCN, Structural Covariance Network; SPM, Statistical Parametric Mapping; STG, Superior Temporal Gyrus; SZ, Schizophrenia; ToM, Theory of Mind; VBM, Voxel-based morphometry.

fronto-temporal regions (Moberget et al., 2018). SCN using anterior insula as a seed reported that the network from each method showed correlations with the neighboring regions strongly and the functional implications were different for each of the methods (Clos et al., 2014). Abbs et al. (2011) selected ACC, PFC, hippocampus, parahippocampal gyrus, and inferior parietal cortex. They reported sex differences in covariance patterns in the inferior parietal lobule, PFC, ACC, and hippocampus. Sex differences in covariance in the inferior parietal lobule-ACC were associated with sex differences in verbal memory performance.

3.2.2.3. SCNs of networks associated with cognitive domains. Examination of cognitive domain networks in first-episode and chronic schizophrenia yielded different results. The first-episode patients but not controls showed positive correlations in executive control network whereas controls but not patients showed positive correlations in auditory regions (Zhang et al., 2020). Chronic patients showed reductions in structural integrity in the fronto-parietal control and salience networks but not in other networks. SCN scores did not correlate with severity of psychopathology (Spreng et al., 2019). These studies examined different sets of networks and used different statistical approaches as well. While Spreng et al. used VBM and PLS on whole-brain, Zhang et al. (2020) used independent correlation analyses by selecting one representative region for each network.

Combining SCN and rsfMRI showed that dysconnectivity in schizophrenia may not be primarily due to DMN dysconnectivity but instead influenced by regions outside the DMN (anterior temporoparietal junction and precuneus). In addition, coupling of the DMN with larger networks to be a problem rather than deficits within the DMN, and a dissociation between structural and functional alterations within the network (Lefort-Besnard et al., 2018).

Deficits in theory of Mind (ToM), a social cognition construct, showed stronger fronto-temporal covariance compared to high ToM group before and after covarying IQ in a surface area-based SCN. Adding medication status as a covariate showed stronger covariance in left caudal MFG and the right MTG in low compared to high ToM group, and left MTG and the left STG in high compared to low ToM group (Raucher-Chéné et al., 2020).

Normative modeling, a novel method to examine SCNs at individual level, involves building a group-level SCN of healthy subjects and then adding one patient at a time to the normative model resulting in a "perturbed SCN" for each patient. *Z*-score of correlation coefficient of perturbed SCN was used to build individual differential SCN (IDSCN) using the Z-scores as the weight of each edge. Using this method, Liu et al. (2021) found the IDSCNs of patients were highly heterogenous, e.g., only 28% of edges were shared by more than one patient. This method revealed greater heterogeneity in the fronto-temporo-parietal network. When group-level SCN was compared with the IDSCNs, each patient contributed differently with small effects whereas accumulated differences contributed more strongly. Despite this heterogeneity, hippocampus-putamen/pallidum edges could subgroup patients and was associated with selected genetic variants.

3.2.2.4. Source based morphometry. SBM revealed finite number of components consisting of highly covarying GM regions. Xu et al. (2009a) reported 5 GM source networks consisting of bilateral temporal, thalamus, basal ganglia, parietal, and frontal-temporal regions, and many WM tracts connecting these regions (Xu et al., 2009b). Compared to VBM, SBM could identify more group differences in regional volume (Kasparek et al., 2010; Xu et al., 2012). Associations with severity of formal thought disorder (Palaniyappan et al., 2015), positive symptoms on PANSS (Gupta et al., 2017) and short-term clinical outcome (Li et al., 2019) were also reported. SBM is proposed to be able to subtype psychosis based on differential association of positive and negative symptoms with IFG and brain stem, respectively (Rahaman et al., 2020). Many regions common to both schizophrenia and bipolar disorder (BD) were identified in the cortical areas suggesting continuum of psychosis (Sorella et al., 2019).

Association of multiple ICs with ECT response (Wolf et al., 2016), earlier onset of cannabis use (Penzel et al., 2021) and inflammation

(Quide et al., 2021) are also reported. SBM identified 25 spatially distinct mostly modestly heritable components; some were associated with 27 linkage disequilibrium-independent genetic variants. Among these, DMN network was associated with schizophrenia (Rodrigue et al., 2020). Another study showed association of SBM-derived heritable insula-MPFC component with SZ (Sprooten et al., 2015).

3.2.2.5. Causality-based structural covariance. An exploration of causality of structural covariance across different durations of illness showed that an increasing duration of illness correlated positively with increasing number of regions showing volume reductions. Jiang et al. (2018) constructed pseudo-time series of GM volume data according to increasing rank of schizophrenia illness duration using the GC model. The volume reduction began in the thalamus as the primary hub of the network with 'causal' progression to volume reductions in a predictable manner to the frontal lobe, then to the temporal and the occipital lobe followed by the cerebellum.

4. Discussion

Structural covariance is a phenomenon where between-subject differences in one region covary with between-subject differences in other regions providing topological information about the brain as a complex network of interconnected regions. Statistically built SCNs can highlight network level abnormalities and altered brain organization underlying a disorder. Published studies have used different statistical approaches to examine SCNs for patient-control differences, and network correlates of cognitive impairments, psychopathology, and outcome. Each study pursued different goals by selecting different sets of brain regions and reported covariance among different regions and correlation with psychopathology and clinical outcome. However, there have been very few attempts to replicate the results, so far. Some studies have examined covariation at the regional level while others have examined the entire brain. No study reported negative findings. For these reasons, it is challenging to meta-analyze these studies. It is unclear if there is a file drawer effect. Despite these shortcomings, recent studies have been focusing on developing novel methods to understand structural covariance in schizophrenia.

Notwithstanding divergent approaches and observed results, certain discernible patterns of covariations in the fronto-temporal, fronto-parietal and thalamofrontal networks with a modest degree of consistency are reported (Breier et al., 1992; Collin et al., 2013; Corradi-Dell'Acqua et al., 2012; Mitelman et al., 2005b; Mitelman et al., 2005c; Niznikiewicz et al., 2000; Portas et al., 1998; Shenton et al., 1992; Wible et al., 2001; Wible et al., 1995). These studies examined hypothesis-based selection of a few regions and whole brain search for volume differences and used correlations and multivariate statistics to report dysconnections in these networks. ROI-based studies have reported altered volume, thickness, and surface area measures in many of the regions included in these networks. Thus, structural covariance highlights differences in within-subject covariation patterns between schizophrenia and controls beyond between-subject regional variations that could help elucidate underlying mechanisms.

There are several inconsistent findings. Initial observations of regional covariations in patients but not in controls (Breier et al., 1992; Shenton et al., 1992) was not supported by later studies that reported different patterns of correlations among controls (Buchanan et al., 2004; Bullmore et al., 1998; Portas et al., 1998), and even stronger correlations in controls than in patients (Woodruff et al., 1997). Such inconsistent findings may have resulted from heterogeneity in the shared variations, not controlling for all covariates or failure to control for the effect of covariation among excluded regions on the selected regions, called conditional correlations in many studies. Shenton et al. (1992) used ICV-corrected volumes whereas Breier et al. (1992) used partial correlations controlling for age and sex. Chen et al. (2014b) regressed out the effects of age, sex, ICV and the volumes of other ROIs not included in the network (conditional correlation), Portas et al. (1998) controlled for ICV, SES and age. Buchanan et al. (2004) adjusted for other volumes examined but not for ICV. Niznikiewicz et al. (2000) used both the raw volumes and ICV-corrected volumes, separately. In addition, correlational approaches to construct a group level network may be affected by the presence of unaccounted latent variables. Further, these studies employed 1.5 and 3 Tesla MRI data with slice thickness between 1.5 mm to 3 mm. Such variations in data acquisition could also affect the morphometric measures and thus the resulting SCNs. Refined parcellations provided different covariation patterns, e.g., while whole thalamic volume did not show covariance with cortical BAs, thalamic nuclei showed interesting patterns of covariance. This suggests that using more refined parcellations could provide more useful information (Mitelman et al., 2005a; Mitelman et al., 2006). This could also suggest that changes in morphometric measurements could affect the SCN patterns.

Inter-regional and inter-lobar covariance examination was an interesting approach. Although interlobar covariance supported fronto-temporal, subcortical-to-frontal and within temporal lobes connectivity, inter-regional covariance was observed across several regions within each lobe (Collin et al., 2013). Maturational deficits were proposed as one of the reasons for interlobar connectivity differences. Bullmore et al. (1998) used SCNs to discriminate between neurodevelopmental and disease-related morphometric changes with some success.

Methodologically sophisticated studies and rigorous designs examining whole brain using advanced statistical approaches such as PCA, PLS, SEM, seed-based network analysis and NBS highlighted the complexity of SCNs in schizophrenia including a possibility of SCN alterations reflecting functional connectivity abnormalities. Spreng et al. (2019) and Zhang et al. (2020) showed stronger structural covariance within selected cognitive brain networks and, structural networks overlapping onto well-established functional network alterations. Although the findings were not fully concordant, the results suggested that the SCNs may not be mere statistical correlations and supported concurrent examination of structural and functional networks to understand the structure-function relationship. Patterns of structural covariance show a complex relationship with functional connectivity (Clos et al., 2014; Lefort-Besnard et al., 2018). Variation in a region could "causally" affect connected regions (Jiang et al., 2018) raising a possibility of volume loss 'spreading' to other regions with disease progression. However, there are several caveats. This study used ranked illness durations that were several years apart as pseudo-time series in a cross-sectional sample. GC applications are used for linear features of signals but "spreading" volumes and disease progression may not be linear. Compensatory mechanisms for volume loss are not considered. Further, GC is not true causality and does not account for latent confounding effects of medications, comorbidities, and pathophysiological processes affecting the disease progression and volume changes. These intriguing findings encourage investigation of schizophrenia as a dysconnection disorder by applying mathematical approaches (see Part II).

Studies examining the clinical significance of SCN alterations related to insight, prognosis and impairments in cognitive domains such as verbal memory, emotion identification and social cognition also do not show concurrence. For example, poor outcome showed different regions with stronger or weaker correlations in different brain regions when different sets of regions are examined using correlational methods (Mitelman et al., 2005b; Mitelman et al., 2005c) and SBM (Li et al., 2019). Regional correlations with severity of hallucinations (Modinos et al., 2009), negative formal thought disorder (Palaniyappan et al., 2015), positive symptoms on PANSS (Gupta et al., 2017) were reported but Spreng et al. (2019) did not find an association of structural covariance scores with psychotic symptom severity. Psychopathology severity evaluated using different scales and sample sizes, variability in psychopathology severity depending on treatment status and illness duration could also have contributed to inconsistencies. Associations with facial emotion detection (Buchy et al., 2017), cognitive insight

(Kuang et al., 2017), and ToM deficits (Raucher-Chéné et al., 2020) have also been reported. Replications are required for these associations.

In summary, published studies report many discernible patterns of correlations and their associations with psychopathology, inflammation, heritability, and cognition that are similar to the ROI-based or whole-brain morphometric studies. However, a major advantage of investigating SCNs is that they highlight topology of these regions and their relationship to the disease and associated clinical variables. Many existing studies have the drawbacks of small sample size, scanner differences, different morphometric measures, e.g., volume and density, and non-uniform control for covariates including treatment interventions; the latter may have complex associations with GM morphometric measures. Medications (Keshavan et al., 1994) and psychotherapy (Eack et al., 2008; Eack et al., 2010) may increase the volume of brain regions, but have not been replicated (Lieberman et al., 2005), and the relationship between amount and duration medications and GM changes is not linear (Roiz-Santiañez et al., 2015). Repeating the analysis with and without medications as a covariate did not yield different results in one study (Collin et al., 2013). More refined gray matter measures such as membrane phospholipid precursor and catabolite levels that index neuronal and glial membrane expansion and contraction in the neuropil also did not show replicated evidence of the association of antipsychotic medications with expansion or contraction of neuropil that contribute to volume (discussed in (Prasad et al., 2016)). A longitudinal MRI study showed brain volume reductions (Ho et al., 2003) that concurs with animal studies (Lewis, 2011). Despite these diverse findings, while controlling for antipsychotic medications should be a standard practice, a better option should be to report both with and without controlling for medications. Recent studies that are methodologically sophisticated should consider strengthening the study designs to address these. Further, guidelines need to be developed to make studies more uniform in their core approaches so that the findings are meta-analyzable.

5. Future directions

An important caveat is that the correlations do not imply causation and hence can lead to spurious impressions of “connection” or “connectedness” in an SCN. Logical next steps include investigation of the extent to which SCN-connectivity maps on to WM connectivity. It is likely that the structure-function relationship will not be linear (Clos et al., 2014; Lefort-Besnard et al., 2018). Studies that clarify such complex relationships could help better explain the meaning of dysconnectivity revealed by the SCNs.

Future studies should examine whole-brain regional covariance by including functional and WM networks employing advanced multivariate statistics to unravel correlational patterns across modalities. Correlations with clinical and cognitive variables using standard scales/batteries are also needed. The discipline of statistical network analysis is witnessing rapid methodological and inferential advances for analyzing graph-structured data and network characteristics encountered in SCNs. Statistical network models could be highly flexible and can capture higher order network structures such as transitivity, reciprocity and assortativity (Loyal and Chen, 2020). Among them stochastic block models and their variants could provide highly flexible approaches to investigate networks (Holland et al., 1983). These methods are beginning to be applied in schizophrenia (Pavlovic et al., 2014). The prospect of applying advanced statistical network analysis techniques - and general random graph models to better understand SCNs and schizophrenia - warrants optimism.

CRediT authorship contribution statement

Dr. Konasale Prasad conceived the idea that was improved by Drs. Jonathan Rubin, Satish Iyengar and Joshua Cape while also contributing to the mathematical (Rubin) and statistical sections (Iyengar and Cape) of the manuscript. Anirban Mitra contributed to the statistical review of methods used in various papers. Nicholas Theis, Brendan Muldoon and Madison Lewis contributed to the review of graph theoretic concepts and figures.

Declaration of competing interest

None of the authors any conflicts of interest that is of direct relevance to the contents of the manuscript.

Acknowledgments

This work was funded through grants from the National Institute of Mental Health R01MH112584 and R01MH115026 (KMP). Funding source did not have any role in determining the content of the manuscript.

References

Abbs, B., Liang, L., Makris, N., Tsuang, M., Seidman, L.J., Goldstein, J.M., 2011. Covariance modeling of MRI brain volumes in memory circuitry in schizophrenia: sex differences are critical. NeuroImage 56 (4), 1865–1874.
Alexander-Bloch, A., Giedd, J.N., Bullmore, E., 2013. Imaging structural co-variance between human brain regions. Nat. Rev. Neurosci. 14 (5), 322–336.
Breier, A., Buchanan, R.W., Elkashef, A., Munson, R.C., Kirkpatrick, B., Gellad, F., 1992. Brain morphology and schizophrenia. A magnetic resonance imaging study of limbic, prefrontal cortex, and caudate structures. Arch. Gen. Psychiatry 49 (12), 921–926.
Buchanan, R.W., Francis, A., Arango, C., Miller, K., Lefkowitz, D.M., McMahon, R.P., Barta, P.E., Pearlson, G.D., 2004. Morphometric assessment of the heteromodal association cortex in schizophrenia. Am. J. Psychiatry 161 (2), 322–331.
Buchy, L., Barbato, M., Makowski, C., Bray, S., MacMaster, F.P., Deighton, S., Addington, J., 2017. Mapping structural covariance networks of facial emotion recognition in early psychosis: a pilot study. Schizophr. Res. 189, 146–152.
Bullmore, E., Sporns, O., 2009. Complex brain networks: graph theoretical analysis of structural and functional systems. Nat. Rev. Neurosci. 10 (3), 186–198.
Bullmore, E., Sporns, O., 2012. The economy of brain network organization. Nat. Rev. Neurosci. 13 (5), 336–349.
Bullmore, E.T., Woodruff, P.W.R., Wright, I.C., Rabe-Hesketh, S., Howard, R.J., Shuriquie, N., Murray, R.M., 1998. Does dysplasia cause anatomical dysconnectivity in schizophrenia? Schizophr. Res. 30 (2), 127–135.
Cannon, T.D., Chung, Y., He, G., Sun, D., Jacobson, A., van Erp, T.G., McEwen, S., Addington, J., Bearden, C.E., Cadenhead, K., Cornblatt, B., Mathalon, D.H., McGlashan, T., Perkins, D., Jeffries, C., Seidman, L.J., Tsuang, M., Walker, E., Woods, S.W., Heinssen, R., <collab>North American Prodrome Longitudinal Study, C.</collab>, 2015. Progressive reduction in cortical thickness as psychosis develops: a multisite longitudinal neuroimaging study of youth at elevated clinical risk. Biol Psychiatry 77 (2), 147–157.
Castro, E., Gupta, C.N., Martinez-Ramon, M., Calhoun, V.D., Arbabshirani, M.R., Turner, J., 2014. Identification of patterns of gray matter abnormalities in schizophrenia using source-based morphometry and bagging. Annu. Int. Conf. IEEE Eng. Med. Biol. Soc. 2014, 1513–1516.
Chan, R.C., Di, X., McAlonan, G.M., Gong, Q.Y., 2011. Brain anatomical abnormalities in high-risk individuals, first-episode, and chronic schizophrenia: an activation likelihood estimation meta-analysis of illness progression. Schizophr. Bull. 37 (1), 177–188.
Chen, J., Liu, J., Calhoun, V.D., Arias-Vasquez, A., Zwiers, M.P., Gupta, C.N., Franke, B., Turner, J.A., 2014a. Exploration of scanning effects in multi-site structural MRI studies. J. Neurosci. Methods 230, 37–50.
Chen, Z., Deng, W., Gong, Q., Huang, C., Jiang, L., Li, M., He, Z., Wang, Q., Ma, X., Wang, Y., Chua, S.E., McAlonan, G.M., Sham, P.C., Collier, D.A., McGuire, P., Li, T., 2014b. Extensive brain structural network abnormality in first-episode treatment-naive patients with schizophrenia: morphometrical and covariation study. Psychol. Med. 44 (12), 2489–2501.
Clos, M., Rottschy, C., Laird, A.R., Fox, P.T., Eickhoff, S.B., 2014. Comparison of structural covariance with functional connectivity approaches exemplified by an investigation of the left anterior insula. NeuroImage 99, 269–280.
Collin, G., de Reus, M.A., Cahn, W., Hulshoff Pol, H.E., Kahn, R.S., van den Heuvel, M.P., 2013. Disturbed grey matter coupling in schizophrenia. Eur. Neuropsychopharmacol. 23 (1), 46–54.
Corradi-Dell'Acqua, C., Tomelleri, L., Bellani, M., Rambaldelli, G., Cerini, R., Pozzi-Mucelli, R., Balestrieri, M., Tansella, M., Brambilla, P., 2012. Thalamic-insular dysconnectivity in schizophrenia: evidence from structural equation modeling. Hum. Brain Mapp. 33 (3), 740–752.
Czepielewski, L.S., Wang, L., Gama, C.S., Barch, D.M., 2017. The relationship of intellectual functioning and cognitive performance to brain structure in schizophrenia. Schizophr. Bull. 43 (2), 355–364.
Dazzan, P., Arango, C., Fleischacker, W., Galderisi, S., Glenthøj, B., Leucht, S., Meyer-Lindenberg, A., Kahn, R., Rujescu, D., Sommer, I., Winter, I., McGuire, P., 2015. Magnetic resonance imaging and the prediction of outcome in first-episode

schizophrenia: a review of current evidence and directions for future research. Schizophr. Bull. 41 (3), 574–583.
DeRamus, T.P., Silva, R.F., Iraji, A., Damaraju, E., Belger, A., Ford, J.M., McEwen, S.C., Mathalon, D.H., Mueller, B.A., Pearlson, G.D., Potkin, S.G., Preda, A., Turner, J.A., Vaidya, J.G., van Erp, T.G.M., Calhoun, V.D., 2020. Covarying structural alterations in laterality of the temporal lobe in schizophrenia: a case for source-based laterality. NMR Biomed. 33 (6), e4294.
Desikan, R.S., Segonne, F., Fischl, B., Quinn, B.T., Dickerson, B.C., Blacker, D., Buckner, R.L., Dale, A.M., Maguire, R.P., Hyman, B.T., Albert, M.S., Killiany, R.J., 2006. An automated labeling system for subdividing the human cerebral cortex on MRI scans into gyral based regions of interest. NeuroImage 31 (3), 968–980.
Eack, S.M., George, M.M., Prasad, K.M., Keshavan, M.S., 2008. Neuroanatomical substrates of foresight in schizophrenia. Schizophr. Res. 103 (1–3), 62–70.
Eack, S.M., Hogarty, G.E., Cho, R.Y., Prasad, K.M., Greenwald, D.P., Hogarty, S.S., Keshavan, M.S., 2010. Neuroprotective effects of cognitive enhancement therapy against gray matter loss in early schizophrenia: results from a 2-year randomized controlled trial. Arch. Gen. Psychiatry 67 (7), 674–682.
Ellison-Wright, I., Glahn, D.C., Laird, A.R., Thelen, S.M., Bullmore, E., 2008. The anatomy of first-episode and chronic schizophrenia: an anatomical likelihood estimation meta-analysis. Am. J. Psychiatry 165 (8), 1015–1023.
van Erp, T.G.M., Walton, E., Hibar, D.P., Schmaal, L., Jiang, W., Glahn, D.C., Pearlson, G. D., Yao, N., Fukunaga, M., Hashimoto, R., Okada, N., Yamamori, H., Bustillo, J.R., Clark, V.P., Agartz, I., Mueller, B.A., Cahn, W., de Zwarte, S.M.C., Hulshoff Pol, H.E., Kahn, R.S., Ophoff, R.A., van Haren, N.E.M., Andreassen, O.A., Dale, A.M., Doan, N. T., Gurholt, T.P., Hartberg, C.B., Haukvik, U.K., Jorgensen, K.N., Lagerberg, T.V., Melle, I., Westlye, L.T., Gruber, O., Kraemer, B., Richter, A., Zilles, D., Calhoun, V.D., Crespo-Facorro, B., Roiz-Santianez, R., Tordesillas-Gutierrez, D., Loughland, C., Carr, V.J., Catts, S., Cropley, V.L., Fullerton, J.M., Green, M.J., Henskens, F.A., Jablensky, A., Lenroot, R.K., Mowry, B.J., Michie, P.T., Pantelis, C., Quide, Y., Schall, U., Scott, R.J., Cairns, M.J., Seal, M., Tooney, P.A., Rasser, P.E., Cooper, G., Shannon Weickert, C., Weickert, T.W., Morris, D.W., Hong, E., Kochunov, P., Beard, L.M., Gur, R.E., Gur, R.C., Satterthwaite, T.D., Wolf, D.H., Belger, A., Brown, G.G., Ford, J.M., Macciardi, F., Mathalon, D.H., O'Leary, D.S., Potkin, S.G., Preda, A., Voyvodic, J., Lim, K.O., McEwen, S., Yang, F., Tan, Y., Tan, S., Wang, Z., Fan, F., Chen, J., Xiang, H., Tang, S., Guo, H., Wan, P., Wei, D., Bockholt, H.J., Ehrlich, S., Wolthusen, R.P.F., King, M.D., Shoemaker, J.M., Sponheim, S.R., De Haan, L., Koenders, L., Machielsen, M.W., van Amelsvoort, T., Veltman, D.J., Assogna, F., Banaj, N., de Rossi, P., Iorio, M., Piras, F., Spalletta, G., McKenna, P.J., Pomarol-Clotet, E., Salvador, R., Corvin, A., Donohoe, G., Kelly, S., Whelan, C.D., Dickie, E.W., Rotenberg, D., Voineskos, A.N., Ciufolini, S., Radua, J., Dazzan, P., Murray, R., Reis Marques, T., Simmons, A., Borgwardt, S., Egloff, L., Harrisberger, F., Riecher-Rossler, A., Smieskova, R., Alpert, K.I., Wang, L., Jonsson, E.G., Koops, S., Sommer, I.E.C., Bertolino, A., Bonvino, A., Di Giorgio, A., Neilson, E., Mayer, A.R., Stephen, J.M., Kwon, J.S., Yun, J.Y., Cannon, D.M., McDonald, C., Lebedeva, I., Tomyshev, A.S., Akhadov, T., Kaleda, V., Fatouros-Bergman, H., Flyckt, L., Karolinska Schizophrenia, P., Busatto, G.F., Rosa, P.G.P., Serpa, M.H., Zanetti, M.V., Hoschl, C., Skoch, A., Spaniel, F., Tomecek, D., Hagenaars, S.P., McIntosh, A.M., Whalley, H.C., Lawrie, S.M., Knochel, C., Oertel-Knochel, V., Stablein, M., Howells, F.M., Stein, D.J., Temmingh, H.S., Uhlmann, A., Lopez-Jaramillo, C., Dima, D., McMahon, A., Faskowitz, J.I., Gutman, B.A., Jahanshad, N., Thompson, P. M., Turner, J.A., 2018. Cortical brain abnormalities in 4474 individuals with schizophrenia and 5098 control subjects via the enhancing neuro imaging genetics through meta analysis (ENIGMA) consortium. Biol. Psychiatry 84 (9), 644–654.
Goodkind, M., Eickhoff, S.B., Oathes, D.J., Jiang, Y., Chang, A., Jones-Hagata, L.B., Ortega, B.N., Zaiko, Y.V., Roach, E.L., Korgaonkar, M.S., Grieve, S.M., Galatzer-Levy, I., Fox, P.T., Etkin, A., 2015. Identification of a common neurobiological substrate for mental illness. JAMA psychiatry 72 (4), 305–315.
Gupta, C.N., Calhoun, V.D., Rachakonda, S., Chen, J., Patel, V., Liu, J., Segall, J., Franke, B., Zwiers, M.P., Arias-Vasquez, A., Buitelaar, J., Fisher, S.E., Fernandez, G., van Erp, T.G., Potkin, S., Ford, J., Mathalon, D., McEwen, S., Lee, H.J., Mueller, B.A., Greve, D.N., Andreassen, O., Agartz, I., Gollub, R.L., Sponheim, S.R., Ehrlich, S., Wang, L., Pearlson, G., Glahn, D.C., Sprooten, E., Mayer, A.R., Stephen, J., Jung, R. E., Canive, J., Bustillo, J., Turner, J.A., 2015. Patterns of gray matter abnormalities in schizophrenia based on an international mega-analysis. Schizophr. Bull. 41 (5), 1133–1142.
Gupta, C.N., Castro, E., Rachkonda, S., van Erp, T.G.M., Potkin, S., Ford, J.M., Mathalon, D., Lee, H.J., Mueller, B.A., Greve, D.N., Andreassen, O.A., Agartz, I., Mayer, A.R., Stephen, J., Jung, R.E., Bustillo, J., Calhoun, V.D., Turner, J.A., 2017. Biclustered independent component analysis for complex biomarker and subtype identification from structural magnetic resonance images in schizophrenia. Front. Psychiatry 8 (179), 179.
Ho, B.C., Andreasen, N.C., Nopoulos, P., Arndt, S., Magnotta, V., Flaum, M., 2003. Progressive structural brain abnormalities and their relationship to clinical outcome: a longitudinal magnetic resonance imaging study early in schizophrenia. Arch. Gen. Psychiatry 60 (6), 585–594.
Holland, P.W., Laskey, K.B., Leinhardt, S., 1983. Stochastic blockmodels: first steps. Soc. Networks 5 (2), 109–137.
Honea, R., Crow, T.J., Passingham, D., Mackay, C.E., 2005. Regional deficits in brain volume in schizophrenia: a meta-analysis of voxel-based morphometry studies. Am. J. Psychiatry 162 (12), 2233–2245.
James, G., Witten, D., Hastle, T., Tibshirani, R., 2013. An Introduction to Statistical Learning. Springer, New York.
Jiang, Y., Luo, C., Li, X., Duan, M., He, H., Chen, X., Yang, H., Gong, J., Chang, X., Woelfer, M., Biswal, B.B., Yao, D., 2018. Progressive reduction in gray matter in patients with schizophrenia assessed with MR imaging by using causal network analysis. Radiology 287 (2), 633–642.
Kasparek, T., Marecek, R., Schwarz, D., Prikryl, R., Vanicek, J., Mikl, M., Ceskova, E., 2010. Source-based morphometry of gray matter volume in men with first-episode schizophrenia. Hum. Brain Mapp. 31 (2), 300–310.
Kennedy, D.N., Lange, N., Makris, N., Bates, J., Meyer, J., Caviness Jr., V.S., 1998. Gyri of the human neocortex: an MRI-based analysis of volume and variance. Cereb. Cortex 8 (4), 372–384.
Keshavan, M.S., Bagwell, W.W., Haas, G.L., Sweeney, J.A., Schooler, N.R., Pettegrew, J. W., 1994. Changes in caudate volume with neuroleptic treatment. Lancet 344 (8934), 1434.
Krishnan, A., Williams, L.J., McIntosh, A.R., Abdi, H., 2011. Partial least squares (PLS) methods for neuroimaging: a tutorial and review. NeuroImage 56 (2), 455–475.
Kuang, C., Buchy, L., Barbato, M., Makowski, C., MacMaster, F.P., Bray, S., Deighton, S., Addington, J., 2017. A pilot study of cognitive insight and structural covariance in first-episode psychosis. Schizophr. Res. 179, 91–96.
Kubera, K.M., Sambataro, F., Vasic, N., Wolf, N.D., Frasch, K., Hirjak, D., Thomann, P.A., Wolf, R.C., 2014. Source-based morphometry of gray matter volume in patients with schizophrenia who have persistent auditory verbal hallucinations. Prog. Neuro-Psychopharmacol. Biol. Psychiatry 50, 102–109.
Lefort-Besnard, J., Bassett, D.S., Smallwood, J., Margulies, D.S., Derntl, B., Gruber, O., Aleman, A., Jardri, R., Varoquaux, G., Thirion, B., Eickhoff, S.B., Bzdok, D., 2018. Different shades of default mode disturbance in schizophrenia: subnodal covariance estimation in structure and function. Hum. Brain Mapp. 39 (2), 644–661.
Lerch, J.P., Worsley, K., Shaw, W.P., Greenstein, D.K., Lenroot, R.K., Giedd, J., Evans, A. C., 2006. Mapping anatomical correlations across cerebral cortex (MACACC) using cortical thickness from MRI. NeuroImage 31 (3), 993–1003.
Lewis, D.A., 2011. Antipsychotic medications and brain volume: do we have cause for concern? Arch. Gen. Psychiatry 68 (2), 126–127.
Li, M., Li, X., Das, T.K., Deng, W., Li, Y., Zhao, L., Ma, X., Wang, Y., Yu, H., Meng, Y., Wang, Q., Palaniyappan, L., Li, T., 2019. Prognostic utility of multivariate morphometry in schizophrenia. Front. Psychiatry 10, 245.
Lieberman, J.A., Tollefson, G.D., Charles, C., Zipursky, R., Sharma, T., Kahn, R.S., Keefe, R.S., Green, A.I., Gur, R.E., McEvoy, J., Perkins, D., Hamer, R.M., Gu, H., Tohen, M., 2005. Antipsychotic drug effects on brain morphology in first-episode psychosis. Arch. Gen. Psychiatry 62 (4), 361–370.
Liu, Z., Palaniyappan, L., Wu, X., Zhang, K., Du, J., Zhao, Q., Xie, C., Tang, Y., Su, W., Wei, Y., Xue, K., Han, S., Tsai, S.J., Lin, C.P., Cheng, J., Li, C., Wang, J., Sahakian, B. J., Robbins, T.W., Zhang, J., Feng, J., 2021. Resolving heterogeneity in schizophrenia through a novel systems approach to brain structure: individualized structural covariance network analysis. Mol. Psychiatry.
Loyal, J.D., Chen, Y., 2020. Statistical network analysis: a review with applications to the coronavirus disease 2019 pandemic. Int. Stat. Rev. 88 (2), 419–440.
Mitelman, S.A., Shihabuddin, L., Brickman, A.M., Hazlett, E.A., Buchsbaum, M.S., 2003. MRI assessment of gray and white matter distribution in Brodmann's areas of the cortex in patients with schizophrenia with good and poor outcomes. Am. J. Psychiatry 160 (12), 2154–2168.
Mitelman, S.A., Brickman, A.M., Shihabuddin, L., Newmark, R., Chu, K.W., Buchsbaum, M.S., 2005a. Correlations between MRI-assessed volumes of the thalamus and cortical Brodmann's areas in schizophrenia. Schizophr. Res. 75 (2–3), 265–281.
Mitelman, S.A., Buchsbaum, M.S., Brickman, A.M., Shihabuddin, L., 2005b. Cortical intercorrelations of frontal area volumes in schizophrenia. NeuroImage 27 (4), 753–770.
Mitelman, S.A., Shihabuddin, L., Brickman, A.M., Buchsbaum, M.S., 2005c. Cortical intercorrelations of temporal area volumes in schizophrenia. Schizophr. Res. 76 (2–3), 207–229.
Mitelman, S.A., Byne, W., Kemether, E.M., Hazlett, E.A., Buchsbaum, M.S., 2006. Correlations between volumes of the pulvinar, centromedian, and mediodorsal nuclei and cortical Brodmann's areas in schizophrenia. Neurosci. Lett. 392 (1–2), 16–21.
Moberget, T., Doan, N.T., Alnaes, D., Kaufmann, T., Cordova-Palomera, A., Lagerberg, T. V., Diedrichsen, J., Schwarz, E., Zink, M., Eisenacher, S., Kirsch, P., Jonsson, E.G., Fatouros-Bergman, H., Flyckt, L., KaSp, Pergola, G., Quarto, T., Bertolino, A., Barch, D., Meyer-Lindenberg, A., Agartz, I., Andreassen, O.A., Westlye, L.T., 2018. Cerebellar volume and cerebellocerebral structural covariance in schizophrenia: a multisite mega-analysis of 983 patients and 1349 healthy controls. Mol Psychiatry 23 (6), 1512–1520.
Modinos, G., Vercammen, A., Mechelli, A., Knegtering, H., McGuire, P.K., Aleman, A., 2009. Structural covariance in the hallucinating brain: a voxel-based morphometry study. J. Psychiatry Neurosci. 34 (6), 465–469.
Niznikiewicz, M., Donnino, R., McCarley, R.W., Nestor, P.G., Iosifescu, D.V., O'Donnell, B., Levitt, J., Shenton, M.E., 2000. Abnormal angular gyrus asymmetry in schizophrenia. Am. J. Psychiatry 157 (3), 428–437.
Padmanabhan, J.L., Tandon, N., Haller, C.S., Mathew, I.T., Eack, S.M., Clementz, B.A., Pearlson, G.D., Sweeney, J.A., Tamminga, C.A., Keshavan, M.S., 2015. Correlations between brain structure and symptom dimensions of psychosis in schizophrenia, schizoaffective, and psychotic bipolar I disorders. Schizophr. Bull. 41 (1), 154–162.
Palaniyappan, L., Mahmood, J., Balain, V., Mougin, O., Gowland, P.A., Liddle, P.F., 2015. Structural correlates of formal thought disorder in schizophrenia: an ultra-high field multivariate morphometry study. Schizophr. Res. 168 (1–2), 305–312.
Pavlovic, Z., Zhu, L., Pereira, L., Singh, R.K., Cornell, R.B., Bakovic, M., 2014. Isoform-specific and protein kinase C-mediated regulation of CTP: phosphoethanolamine cytidylyltransferase phosphorylation. J. Biol. Chem. 289 (13), 9053–9064.
Penzel, N., Antonucci, L.A., Betz, L.T., Sanfelici, R., Weiske, J., Pogarell, O., Cumming, P., Quednow, B.B., Howes, O., Falkai, P., Upthegrove, R., Bertolino, A., Borgwardt, S., Brambilla, P., Lencer, R., Meisenzahl, E., Rosen, M., Haidl, T., Kambeitz-Ilankovic, L., Ruhrmann, S., Salokangas, R.R.K., Pantelis, C., Wood, S.J.,

Koutsouleris, N., Kambeitz, J., Consortium, P., 2021. Association between age of cannabis initiation and gray matter covariance networks in recent onset psychosis. Neuropsychopharmacology. https://doi.org/10.1038/s41386-021-00977-9.
Portas, C.M., Goldstein, J.M., Shenton, M.E., Hokama, H.H., Wible, C.G., Fischer, I., Kikinis, R., Donnino, R., Jolesz, F.A., McCarley, R.W., 1998. Volumetric evaluation of the thalamus in schizophrenic male patients using magnetic resonance imaging. Biol. Psychiatry 43 (9), 649–659.
Prasad, K.M., Patel, A.R., Muddasani, S., Sweeney, J., Keshavan, M.S., 2004a. The entorhinal cortex in first-episode psychotic disorders: a structural magnetic resonance imaging study. Am. J. Psychiatry 161 (9), 1612–1619.
Prasad, K.M., Rohm, B.R., Keshavan, M.S., 2004b. Parahippocampal gyrus in first episode psychotic disorders: a structural magnetic resonance imaging study. Prog. Neuro-Psychopharmacol. Biol. Psychiatry 28 (4), 651–658.
Prasad, K.M., Sahni, S.D., Rohm, B.R., Keshavan, M.S., 2005. Dorsolateral prefrontal cortex morphology and short-term outcome in first-episode schizophrenia. Psychiatry Res. 140 (2), 147–155.
Prasad, K.M., Goradia, D., Eack, S., Rajagopalan, M., Nutche, J., Magge, T., Rajarethinam, R., Keshavan, M.S., 2010. Cortical surface characteristics among offspring of schizophrenia subjects. Schizophr. Res. 116 (2–3), 143–151.
Prasad, K.M., Burgess, A., Nimgaonkar, V.L., Keshavan, M.S., Stanley, J.A., 2016. Neuropil pruning in early-course schizophrenia: immunological, clinical and neurocognitive correlates. Biol.Psychiatry 1 (6), 528–538.
Quide, Y., Matosin, N., Atkins, J.R., Fitzsimmons, C., Cairns, M.J., Carr, V.J., <collab>Australian Schizophrenia Research, B.</collab>, Green, M.J., 2018. Common variation in ZNF804A (rs1344706) is not associated with brain morphometry in schizophrenia or healthy participants. Prog Neuropsychopharmacol Biol Psychiatry 82, 12–20.
Quide, Y., Bortolasci, C.C., Spolding, B., Kidnapillai, S., Watkeys, O.J., Cohen-Woods, S., Carr, V.J., Berk, M., Walder, K., Green, M.J., 2021. Systemic inflammation and grey matter volume in schizophrenia and bipolar disorder: moderation by childhood trauma severity. Prog. Neuro-Psychopharmacol. Biol. Psychiatry 105, 110013.
Rahaman, M.A., Turner, J.A., Gupta, C.N., Rachakonda, S., Chen, J., Liu, J., Erp, T.G.M. V., Potkin, S., Ford, J., Mathalon, D., Lee, H.J., Jiang, W., Mueller, B.A., Andreassen, O., Agartz, I., Sponheim, S.R., Mayer, A.R., Stephen, J., Jung, R.E., Canive, J., Bustillo, J., Calhoun, V.D., 2020. N-BiC: A Method for Multi-Component and Symptom Biclustering of Structural MRI Data: Application to Schizophrenia. IEEE Transactions on Biomedical Engineering 67 (1), 110–121.
Raucher-Chéné, D., Lavigne, K.M., Makowski, C., Lepage, M., 2020. Altered surface area covariance in the mentalizing network in schizophrenia: insight into theory of mind processing. Biol Psychiatry Cogn Neurosci Neuroimaging. https://doi.org/10.1016/j.bpsc.2020.06.020.
Rodrigue, A.L., Alexander-Bloch, A.F., Knowles, E.E.M., Mathias, S.R., Mollon, J., Koenis, M.M.G., Perrone-Bizzozero, N.I., Almasy, L., Turner, J.A., Calhoun, V.D., Glahn, D.C., 2020. Genetic contributions to multivariate data-driven brain networks constructed via source-based morphometry. Cereb. Cortex 30 (9), 4899–4913.
Roiz-Santiañez, R., Suarez-Pinilla, P., Crespo-Facorro, B., 2015. Brain structural effects of antipsychotic treatment in schizophrenia: a systematic review. Curr. Neuropharmacol. 13 (4), 422–434.
Shenton, M.E., Kikinis, R., Jolesz, F.A., Pollak, S.D., LeMay, M., Wible, C.G., Hokama, H., Martin, J., Metcalf, D., Coleman, M., et al., 1992. Abnormalities of the left temporal lobe and thought disorder in schizophrenia. A quantitative magnetic resonance imaging study. N. Engl. J. Med. 327 (9), 604–612.
Shenton, M.E., Dickey, C.D., Frumin, M., McCarley, R.W., 2001. A review of MRI findings in schizophrenia. Schizophr. Res. 49, 1–52.
Sorella, S., Lapomarda, G., Messina, I., Frederickson, J.J., Siugzdaite, R., Job, R., Grecucci, A., 2019. Testing the expanded continuum hypothesis of schizophrenia and bipolar disorder. Neural and psychological evidence for shared and distinct mechanisms. NeuroImage: Clin. 23, 101854.
Spreng, R.N., DuPre, E., Ji, J.L., Yang, G., Diehl, C., Murray, J.D., Pearlson, G.D., Anticevic, A., 2019. Structural covariance reveals alterations in control and salience network integrity in chronic schizophrenia. Cereb. Cortex 29 (12), 5269–5284.
Sprooten, E., Gupta, C.N., Knowles, E.E., McKay, D.R., Mathias, S.R., Curran, J.E., Kent Jr., J.W., Carless, M.A., Almeida, M.A., Dyer, T.D., Goring, H.H., Olvera, R.L., Kochunov, P., Fox, P.T., Duggirala, R., Almasy, L., Calhoun, V.D., Blangero, J., Turner, J.A., Glahn, D.C., 2015. Genome-wide significant linkage of schizophrenia-related neuroanatomical trait to 12q24. Am. J. Med. Genet. B Neuropsychiatr. Genet. 168 (8), 678–686.
Steen, R.G., Mull, C., McClure, R., Hamer, R.M., Lieberman, J.A., 2006. Brain volume in first-episode schizophrenia: systematic review and meta-analysis of magnetic resonance imaging studies. Br. J. Psychiatry 188, 510–518.
Stephan, K.E., Friston, K.J., Frith, C.D., 2009. Dysconnection in schizophrenia: from abnormal synaptic plasticity to failures of self-monitoring. Schizophr. Bull. 35 (3), 509–527.
Suarez, L.E., Markello, R.D., Betzel, R.F., Misic, B., 2020. Linking structure and function in macroscale brain networks. Trends Cogn. Sci. 24 (4), 302–315.
Turner, J.A., Calhoun, V.D., Michael, A., van Erp, T.G., Ehrlich, S., Segall, J.M., Gollub, R.L., Csernansky, J., Potkin, S.G., Ho, B.C., Bustillo, J., Schulz, S.C., Fbirn, Wang, L., 2012. Heritability of multivariate gray matter measures in schizophrenia. Twin research and human genetics : the official journal of the International Society for Twin Studies 15 (3), 324–335.
Vita, A., De Peri, L., Silenzi, C., Dieci, M., 2006. Brain morphology in first-episode schizophrenia: a meta-analysis of quantitative magnetic resonance imaging studies. Schizophr. Res. 82 (1), 75–88.
Wheeler, A.L., Chakravarty, M.M., Lerch, J.P., Pipitone, J., Daskalakis, Z.J., Rajji, T.K., Mulsant, B.H., Voineskos, A.N., 2014. Disrupted prefrontal interhemispheric structural coupling in schizophrenia related to working memory performance. Schizophr. Bull. 40 (4), 914–924.
Wible, C.G., Shenton, M.E., Hokama, H., Kikinis, R., Jolesz, F.A., Metcalf, D., McCarley, R.W., 1995. Prefrontal cortex and schizophrenia. A quantitative magnetic resonance imaging study. Arch. Gen. Psychiatry 52 (4), 279–288.
Wible, C.G., Anderson, J., Shenton, M.E., Kricun, A., Hirayasu, Y., Tanaka, S., Levitt, J.J., O'Donnell, B.F., Kikinis, R., Jolesz, F.A., McCarley, R.W., 2001. Prefrontal cortex, negative symptoms, and schizophrenia: an MRI study. Psychiatry Res. 108 (2), 65–78.
Wolf, R.C., Nolte, H.M., Hirjak, D., Hofer, S., Seidl, U., Depping, M.S., Stieltjes, B., Maier-Hein, K., Sambataro, F., Thomann, P.A., 2016. Structural network changes in patients with major depression and schizophrenia treated with electroconvulsive therapy. Eur. Neuropsychopharmacol. 26 (9), 1465–1474.
Wolf, R.C., Rashidi, M., Fritze, S., Kubera, K.M., Northoff, G., Sambataro, F., Calhoun, V. D., Geiger, L.S., Tost, H., Hirjak, D., 2020. A neural signature of parkinsonism in patients with schizophrenia Spectrum disorders: a multimodal MRI study using parallel ICA. Schizophr. Bull. 46 (4), 999–1008.
Woodruff, P.W., Wright, I.C., Shuriquie, N., Russouw, H., Rushe, T., Howard, R.J., Graves, M., Bullmore, E.T., Murray, R.M., 1997. Structural brain abnormalities in male schizophrenics reflect fronto-temporal dissociation. Psychol. Med. 27 (6), 1257–1266.
Wright, I.C., Sharma, T., Ellison, Z.R., McGuire, P.K., Friston, K.J., Brammer, M.J., Murray, R.M., Bullmore, E.T., 1999. Supra-regional brain systems and the neuropathology of schizophrenia. Cereb. Cortex 9 (4), 366–378.
Xu, L., Groth, K.M., Pearlson, G., Schretlen, D.J., Calhoun, V.D., 2009a. Source-based morphometry: the use of independent component analysis to identify gray matter differences with application to schizophrenia. Hum. Brain Mapp. 30 (3), 711–724.
Xu, L., Pearlson, G., Calhoun, V.D., 2009b. Joint source based morphometry identifies linked gray and white matter group differences. NeuroImage 44 (3), 777–789.
Xu, L., Adali, T., Schretlen, D., Pearlson, G., Calhoun, V.D., 2012. Structural angle and power images reveal interrelated gray and white matter abnormalities in schizophrenia. Neurol. Res. Int. 2012, 735249.
Zalesky, A., Fornito, A., Bullmore, E.T., 2010. Network-based statistic: identifying differences in brain networks. NeuroImage 53 (4), 1197–1207.
Zalesky, A., Pantelis, C., Cropley, V., Fornito, A., Cocchi, L., McAdams, H., Clasen, L., Greenstein, D., Rapoport, J.L., Gogtay, N., 2015. Delayed development of brain connectivity in adolescents with schizophrenia and their unaffected siblings. JAMA Psychiatry 72 (9), 900–908.
Zhang, X., Liu, W., Guo, F., Li, C., Wang, X., Wang, H., Yin, H., Zhu, Y., 2020. Disrupted structural covariance network in first episode schizophrenia patients: evidence from a large sample MRI-based morphometric study. Schizophr. Res. 224, 24–32.